https://doi.org/10.5194/egusphere-2026-4356
Preprint. Discussion started: 18 August 2026


# A High-Resolution Continuous Melter System for Sea Ice and Sediment-Laden Ice Applications

Rafael dos Reis[1†], Denise Mondragon[1†], Nolan Magner[1], Bruce Vaughn[2], Valerie Morris[2], Kevin Hand[3], Catherine Walker[4], Christopher R. German[5], Joseph McConnell[6], Helle Astrid Kjær[7], Melisa Diaz[1]

[1]School of Earth Sciences, The Ohio State University, 43210, Columbus-OH, USA.
[2]Institute of Arctic and Alpine Research, University of Colorado, 80309, Boulder-CO, USA
[3]Jet Propulsion Laboratory, California Institute of Technology,91109, Pasadena-CA, USA
[4]Department of Applied Ocean Physics and Engineering, Woods Hole Oceanographic Institution, 02543, Woods Hole-MA, USA
[5]Department of Geology & Geophysics, Woods Hole Oceanographic Institution, 02543, Woods Hole-MA, USA
[6]Division of Hydrologic Sciences, Desert Research Institute, 89512, Reno, NV, USA
[7]Physics of Ice, Climate and Earth (PICE), Niels Bohr Institute, University of Copenhagen, Copenhagen, Denmark
†co-first authors

*Correspondence to*: Rafael dos Reis (dosreis.3@osu.edu)

**Abstract.** Sea ice cores preserve a stratified record of biogeochemical processes that are central to understanding coupled ocean–ice–atmosphere processes. Previously, continuous melter systems were optimized for relatively clean glacial ice and perform poorly on sediment-laden sea ice. Here we present a new high-resolution continuous melter system specifically engineered for sea ice applications. This system combines capabilities of full core processing, inline filtration, and ice depth-resolution control. Further, this configuration allows simultaneous processing of inner and outer meltwater streams, collection of varied grain size fractions, and control for custom user-defined depth resolution during discrete sample collection. Validation experiments using artificial ice cores spanning sea ice densities (~0.7–0.9 g $cm^{-3}$) presented reproducible volume collection, salinity boundaries preservation at sub-centimeter scales, low memory effects (typically <10%), and high sediment recovery of ~86% across a 1–106 µm size range. These results show that the new system presented here provides high-resolution discrete sampling of both dissolved and particulate phases, overcoming limitations of existing continuous melter system's approaches for sediment-rich sea ice cores. With this advancement, new high-resolution analysis for sea ice can be achieved for biogeochemical and paleoclimate reconstructions in polar environments.

## 1 Introduction

Sea ice is an important and understudied component of the cryosphere that covers approximately 20% of the Earth's surface and creates a barrier between the atmosphere and the ocean (Fountain et al., 2012), thereby acting as an archive of both atmospheric and oceanic processes. Sea ice accumulates aerosols, mineral dust, and anthropogenic contaminants through atmospheric deposition and acquires nutrients, elements, and particles via riverine and oceanic inputs (Miller et al., 2015; Pradel et al., 2025). As such, sea ice also serves as an important archive of ocean circulation, the evolution of ocean biogeochemical processes, marine ecosystem dynamics, and chemical/physical proxies useful

https://doi.org/10.5194/egusphere-2026-4356
Preprint. Discussion started: 18 August 2026


for reconstructing polar climate dynamics (Abram et al., 2013; Eayrs et al., 2021; Fadeev et al., 2021; Wang et al., 2014; Winski et al., 2021).

Sea ice is increasingly threatened by rapid climate change (Willis et al., 2023). Arctic Sea ice is becoming thinner, younger, and more ephemeral, likely caused by polar amplification and anthropogenic effects (Stroeve and Notz, 2018; Willis et al., 2023). As a result, although sea ice is an informative archive of atmospheric and oceanic processes, it is also a vulnerable one, and its capacity to record environmental change is likely to become progressively compromised under continued warming (Meier and Stroeve, 2022).

Sea ice formation involves the freezing of ocean water, where salt rejection can generate a network of brine channels that store dissolved salts and nutrients (e.g., $Na^+$, $Ca^{2+}$, $Mg^{2+}$, $K^+$, $Cl^-$, $NO_3^-$, and $SO_4^{2-}$), organic matter, and fine silt and clay sediment (Fripiat et al., 2014). Previous analyses (Arrigo, 2014; Duprat et al., 2020) observed that these nutrients, dissolved salts, and sediments are cryo-concentrated, predominately, at the bottom of the sea ice in a region hosting diverse microorganism communities (Frantz et al., 2026; Tedesco and Vichi, 2014). During melting seasons, these solutes (dissolved salts and nutrients) can sustain up to 35% of total primary production in some regions, like the Southern Ocean, significantly impacting biogeochemical cycling and pollutant transport in polar oceans (Eicken et al., 2005; Lizotte, 2001; Wegner et al., 2017). Recent changes in sea ice extent have altered biogeochemical cycling, leading to an increased supply of nutrients, including the micronutrient iron, and other dissolved solutes to the surface ocean (Lannuzel et al., 2016). These processes highlight the impact that changes in polar climate dynamics have on our oceans and how sea ice cores can be used to predict future solute and sediment fluxes to the ocean (Parkinson, 2019; Turner et al., 2020).

Sea ice cores also provide a framework for understanding chemically dynamic ice–ocean systems beyond Earth. In the Arctic Ocean, sea ice formation and breakup regulate exchanges between the ocean and ice, while its internal chemistry reflects the movement of dissolved solutes and particulates (Bacon, 2023; Fripiat et al., 2014). Because comparable ice-ocean (±atmosphere) processes may occur in the subsurface oceans of icy ocean worlds (e.g. Europa and Enceladus), sea ice is also often used as an analog for the study of habitability, brine chemistry, and through-ice transport of dissolved nutrients and solutes in those extraterrestrial settings (Martin and McMinn, 2018).

To date, studying sea ice cores has been difficult. Unlike pristine ice cores from polar ice sheet interiors, that are typically low in solutes and sediment load, sea ice cores often contain highly variable sediment loads (i.e. 1.3–306 mg/L of sediment, Nürnberg et al., 1994) and high salt concentrations (i.e., 32-46 Practical Salinity Unit –PSU, Tedesco and Vichi, 2014) which makes them challenging to assess with the same methods and techniques. Therefore, in most studies sea ice cores have been processed using the previously established discrete techniques: (i) mechanical removal of the outer core under clean conditions (e.g. ISO 14644-1 Class 1 clean room), (ii) sectioning into 5–10 cm segments, and (iii) melting each segment as a bulk sample in pre-cleaned bottles for aqueous analysis (e.g. (Geilfus et al., 2021; Lange et al., 2023; Lenss et al., 2025). Although widely applied, this workflow can result in ice-loss during the sectioning process and is time-consuming, labor-intensive, and inherently limits high spatial- (hence, temporal-) resolution studies. By contrast, continuous melter systems offer an alternative to manual processing and can deliver high-resolution profiles (down to sub-centimeter scales). However, existing systems (see section 2.1 for full system

https://doi.org/10.5194/egusphere-2026-4356
Preprint. Discussion started: 18 August 2026


overview) were not developed to process sediment-laden sea ice cores, which are often considered too complexly matrixed and heterogeneous with respect to density, for routine continuous-flow processing.

To address these limitations, we have developed a new high-resolution continuous melter system, the Ice Core Analysis for Research and Understanding of Sea-ice (ICARUS) melter system, that is specifically engineered for highly impure sea ice cores. In this study, we evaluate its performance for volume stability, vertical preservation, carryover, and particulate recovery. This melter system expands the range of geochemical and isotopic information that can be recovered from sea ice cores through depth-resolved sampling of both dissolved and particulate phases. Although motivation for the design of ICARUS was to analyze sea ice cores more effectively, the system is also capable of handling sediment-laden glacier ice, broadening its applicability to future cryosphere–climate studies.

## 2. Melter System Overview

Two main classes of continuous melter systems (Fig. 1) are currently used for ice-core analysis: Continuous Flow Analysis (CFA) and Continuous Melting with Discrete Sampling (CMDS). Both approaches have enabled high-resolution measurements on glacial ice by respectively directing meltwater either directly to analytical instruments or fraction collectors (Osterberg et al., 2006; Röthlisberger et al., 2000; Sigg et al., 1994). Hybrid CFA/CMDS systems also exist that combine full CFA analyses with routine and systematic capture of both acidified and unacidified discrete meltwater samples for later offline analysis (McConnell et al., 2017).

In all cases, continuous melter systems have substantially reduced manual handling and associated contamination risks compared to traditional sectioning. The CFA and CMDS architectures, however, involve distinct trade-offs for high-resolution ice core analysis (see section 2.1 for examples).

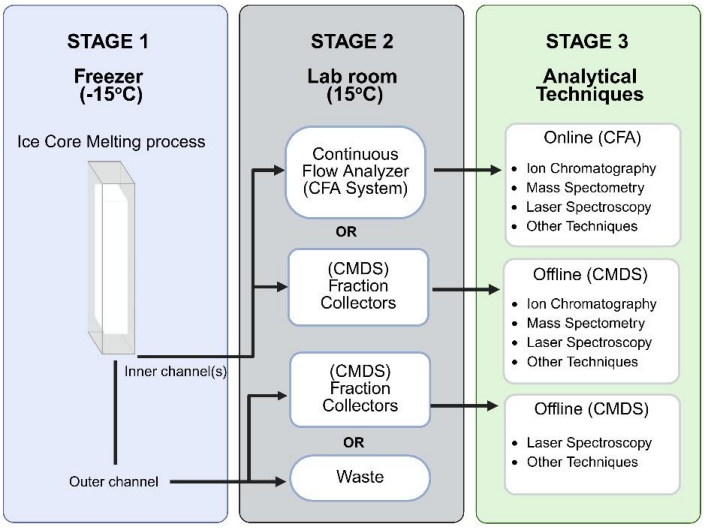


**Figure 1. Schematic of a continuous ice-core melting system in three stages, illustrating meltwater flow path from inner and outer channels to either online CFA or discrete CMDS collection and subsequent application of analytical techniques online**

https://doi.org/10.5194/egusphere-2026-4356
Preprint. Discussion started: 18 August 2026


**or offline. Stage 1) meltwater flow path from inner and outer channels; Stage 2) CFA or discrete CMDS collection; Stage 3) subsequent application of analytical techniques online or offline.**

### 2.1. Existing Systems

Since the first CFA melter systems were introduced in the early 1990's (Fuhrer et al., 1993; Sigg et al., 1994), designs have been progressively adapted to address different ice-core challenges and increasingly complex analytical requirements. CFA systems have allowed continuous measurements of chemical and isotopic data at centimeter and sometimes sub-centimeter scales while preserving the integrity of analytes (Dallmayr et al., 2025; Emanuelsson et al., 2015). First introduced by Sigg et al. (1994), CFA systems were used to measure a specific group of ions and compounds, including $H_2O_2$, $NH_4^+$, $Ca^+$, and $NO_3^-$, using fluorimetry and absorption spectroscopy. Later, direct coupling of an ice core melter with a traditional CFA system to an inductively coupled plasma mass spectrometer (ICP-MS) provided additional continuous measurements of 11 major and trace elements (i.e., Na, Mg, Al, K, Mn, Rb, Sr, Zr, Ba, Nd, Pb; McConnell et al., 2002). This system was soon modified to include two Sector Field Mass Spectrometers (SFMS) instruments operating in parallel that increased the number of elements that could be measured and lowered detection limits substantially (McConnell et al., 2017). Modernized systems also have introduced new high speed/resolution multi-ion analysis, such as pseudo-continuous Ion chromatography (Cole-Dai et al., 2006) and other specialized instrument analyses, including multi-element trace metals and biomass-burning markers (Grieman et al., 2018; McConnell et al., 2007), while maintaining continuous melting. Subsequent developments expanded CFA capabilities to include stable water isotope measurements (e.g., $d^{18}O$) to integrate fraction collectors for CMDS (Emanuelsson et al., 2015; Gkinis et al., 2010, 2011; Jones et al., 2017; Maselli et al., 2013).

CMDS systems have provided flexibility with sample use since their introduction in the 2000's, allowing different preservation techniques and enabling precise multi-elemental analyses from one core (Osterberg et al., 2006). Further innovation of CFA systems has led to the development of the first lightweight in situ analysis (LISA) box, a portable CFA setup capable of operating in extreme field conditions and measuring $H_2O_2$ (Kjær et al., 2021). Currently, both types of systems are capable of analysis at high-resolution and for a broad analytical range (see Table 1).

Many CFA and CMDS systems employ a dual-channel melt head design (see fig. 3; Osterberg et al., 2006; Sigg et al., 1994). An inner channel (typically 70 to 80% of the sample cross section) is dedicated to producing uncontaminated meltwater for geochemical analysis, while an outer channel collects less pristine meltwater that is typically discarded or used for less contamination-sensitive analyses (Bigler et al., 2011; Tetzner et al., 2025). For continuous ultra-trace-level measurements, the most advanced melt heads divide the meltwater stream into three regions (McConnell et al., 2017). In such systems, only the inner-most 10% of the meltwater stream is processed for ultra-trace measurements using one or more Sector Field Inductively Coupled Mass Spectrometers (SF-ICPMS), the next 20% is used for more traditional CFA determinations such as ammonium, nitrate, hydrogen peroxide, stable water isotopes, and refractory black carbon, and the outer 70% either discarded or captured for measurements of parameters that are not easily contaminated and require large sample volumes (e.g., $^{10}Be$ and volcanic tephra, McConnell et al., 2017).

In a typical configuration, a temperature-controlled melt head housed inside a freezer contacts the base of a vertically oriented ice core, melting it at a controlled rate while the top of the core remains frozen (McConnell et al., 2002). The

https://doi.org/10.5194/egusphere-2026-4356
Preprint. Discussion started: 18 August 2026


melt head temperature is regulated by heat cartridges and a precision thermoregulator to maintain a stable melt rate and uniform heat distribution. The melt head devices are usually constructed from thermally conductive, chemically inert materials such as aluminum or copper (McConnell et al., 2002), and are further protected by electroless nickel plating and/or a protective gold coating to prevent trace metal contamination (Bigler et al., 2011; McConnell et al., 2002; Osterberg et al., 2006; Röthlisberger et al., 2000; Sigg et al., 1994). Aluminum and copper from the melthead, as well as nickel and gold solutions used for plating, all contain impurities such as base metals that contaminate the meltwater stream. Therefore, continuous melter systems designed specifically for ultra-trace-level measurements use melt heads made from inert ceramic materials such as silica carbide, thereby eliminating release of any impurities and allowing routine cleaning of the melter system with ultra-pure acid (McConnell et al., 2017). After contacting the melt head, meltwater is transported through polyethylene tubing to either analytical detectors (CFA) or fraction collectors (CMDS). For ultra-trace applications, Teflon tubing is used throughout the melt water flow path instead (McConnell et al. 2017). Additionally, some melter systems may use debubblers to remove trapped air or gas from the melt stream in the tubing before it reaches sensitive equipment downstream (e.g. Dallmayr et al., 2025).

**Table 1. Summary of continuous melting and analytical system configurations utilized in major ice-core laboratories over the past ~30 years. Depth-resolution values represent typical operational ranges and depend strongly on the analyte measured, the coupled analytical instruments and the physical properties (density and porosity) of the ice or firn being melted. Melt rates correspond to typical operational regimes reported in the cited studies.**

| Location | System type | Melt Head | Melt rate ($cm.min^{-1}$) | Depth resolution (cm) | Key References |
|---|---|---|---|---|---|
| University of Bern | CFA / Field–campaign CFA / CFA + ICP-TOFMS | Solid Al / Cu plated with electroless Ni (5 µm) and Au (2 µm). | 4 / ~3.5 | ~1/ ~0.8–10 | (Sigg et al., 1994; Röthlisberger et al., 2000; Kaufmann et al., 2008; Erhardt et al., 2019, 2023). |
| Desert Research Institute | CFA + dual SF-ICPMS + CMDS | Chemically inert ceramic | ~3–6 | 0.2–2 | (McConnell et al., 2002, 2017) |
| University of Maine | CMDS | Al base with Ni270 melter plate | 1.5 − 3 | ~1–2 | (Osterberg et al., 2006) |

https://doi.org/10.5194/egusphere-2026-4356
Preprint. Discussion started: 18 August 2026


| | | | | | |
|---|---|---|---|---|---|
| University of Copenhagen | CFA / portable CFA (LISA Box) | Cu plated with electroless Ni and Au / Solid Al | 1.5 / ~1–2 | ~0.8–2.5 / ~1 | (Bigler et al., 2011; Kjær et al., 2021; Simonsen et al., 2019; Winstrup et al., 2019) |
| University of Florence | CFA + FIC | Al surface-coated with PTFE | 4 | ~ 1.0 | (Severi et al., 2015) |
| NIPR (Japan) | CFA | Cu plated with electroless Ni and Au | ~3–4 | ~1–4 | (Dallmayr et al., 2016, 2025; Goto-Azuma et al., 2024) |
| University of Colorado | CFA-CRDS | Solid Al | ~2.5 | ~ 1 | (Jones et al., 2017) |
| British Antarctic Survey | CFA | Cu plated with electroless Ni and Au | ~3.0 | ~1.4–4.0 | (Grieman et al., 2022) |
| Ca' Foscari Venice | CFA + FLC-MS/MS | Solid Al | ~3–4 | ~1 | (Spagnesi et al., 2023) |
| This study | CMDS | Al base coated with electroless Ni and Au; Al base coated with FEP | 0.5–1.4 | ≥ 0.5 | Dos Reis et al. (this study) |

### 2.2. Analytical Techniques for Continuous Melter Systems

While CFA-based systems provide high-resolution capabilities for clean glacial ice, sediment-laden matrices like sea ice present analytical constraints. Below, we present the limitations of CFA-based approaches and describe how CMDS systems can address them by examining three major analytical techniques which have been most often applied to continuous melter systems with discrete sampling.

#### 2.2.1. Chromatography

Ion Chromatography (IC) coupled to CFA systems has provided unprecedented high-resolution measurement of selected major ions (e.g., $Cl^-$, $NO_3^-$, $SO_4^{2-}$) in ice cores (Huber et al., 2001; Morganti et al., 2007; Traversi et al., 2002). Subsequent advances to increase the injection frequency, including Ultra-Fast Ion Chromatography (Severi et al., 2015) and addition of more IC's have been implemented, while Fast Liquid Chromatography-Mass Spectrometry has extended the technique to trace organic analytes (Barbaro et al., 2022; Spagnesi et al., 2023). Gas Chromatography coupled with Flame Ionization Detection has also been incorporated for the semicontinuous, field-deployable measurement of methane ($CH_4$) in ice cores (Federer et al., 2009). More recently, continuous measurements of methane, carbon monoxide and nitrous oxide using cavity ring-down spectroscopy have largely superseded GC–FID

https://doi.org/10.5194/egusphere-2026-4356
Preprint. Discussion started: 18 August 2026


approaches and are now routinely deployed for both laboratory and field ice-core gas analyses (Faïn et al., 2014; Rhodes et al., 2015). However, CFA-IC analysis can only measure dissolved ionic species in meltwater. Sea ice cores contain elevated particulate loads (including marine salt particles and biogenic particulates) that can clog detectors and complicate in-line measurements. Particulate phase analytes are not captured by CFA-IC systems, excluding important data.

#### 2.2.2. Mass spectrometry: Trace Element and Multi-Elemental Analysis

CFA-ICP-MS systems enabled high-resolution measurements of elements and chemical species at the parts per billion (ppb) and parts per trillion (ppt) levels (Knüsel et al., 2003; McConnell et al., 2002) and in some cases measurement resolution can range from low- to mid- parts per quadrillion (ppq) range (McConnell et al., 2017). Quadrupole Mass Spectrometry (QMS), Sector Field Mass Spectrometry (SFMS), and Inductively Coupled Plasma Optical Emission Spectroscopy (ICP-OES) were initially deployed as ICP detectors for continuous melter systems (Knüsel et al., 2003; McConnell et al., 2002). The SFMS became the preferred option for applications requiring higher resolution and accuracy (Uglietti et al., 2014; Vallelonga et al., 2021) and for very low elemental concentrations (McConnell et al., 2017). Most recently, CFA-Time-of-Flight MS (TOFMS) systems enabled simultaneous measurement of all analyte masses and detection of multi-elemental fast transient signals at unprecedented temporal resolution (Erhardt et al., 2019, 2023). Although this high-resolution trace and multi elemental measurements can be made using CFA-ICP-MS analysis, they are constrained by brief meltwater transit time (minutes) often leading to insufficient acidification time necessary for complete particulate dissolution. While recovery is 100% for more soluble compounds such as volcanic sulfur, sea salt, carbonate dust, and industrial pollutants, this relatively short transit time sometimes results in 50-90% recovery for some elements (i.e., Ca, Cd, Ce, Gd, Mg, Mn, Sm, U, V, and Yb) and <50% for others (i.e. Al, Fe, and La) compared to discrete analyses with extended acidification depending on the relative amounts of recalcitrant material such as aluminus dust (≥3 months; Arienzo et al., 2019). This results in the underestimation of proxy signals although methods to determine and correct for under-recovery are routine. For sea ice cores, where elevated sediment presence can potentially comprise a substantial fraction, discrete sampling enables extended acidification protocols.

#### 2.2.3. Laser spectroscopy

Laser Absorption Spectrometry (LAS) is another technique coupled to CFA and applied to measure hydrogen ($\delta D$) and oxygen ($\delta^{18}O$) isotope ratios (Gkinis et al., 2010) by both Wavelength Scanned-Cavity Ring-Down Spectroscopy (WS-CRDS) and Off-Axis Integrated Cavity Output Spectroscopy (OA-ICOS). OA-ICOS provides accurate measurements at high concentrations, while WS-CRDS demonstrates greater stability for secondary parameters such as d-excess and $^{17}O$-excess (Emanuelsson et al., 2015). Recently, continuous and simultaneous coupling of two WS-CRDS instruments have been set up with CFA (Steig et al., 2021).

Similar to other techniques coupled with CFA, these systems face a critical constraint related to internal mixing within the continuous flow system. This causes displacement of water molecules from their original positions in the ice matrix, resulting in signal smoothing and attenuation of fine-scale isotopic variability (Gkinis et al., 2010; Petteni et al., 2025). For sea ice cores, this limitation is particularly critical, especially where salt-enriched alternating

https://doi.org/10.5194/egusphere-2026-4356
Preprint. Discussion started: 18 August 2026


layers of ice and particulate-rich melt preserve sub-centimeter biogeochemical information. Additionally, the high particulate loads in sea ice might cause melt-rate variability during continuous melting, altering integration times and compromising precision for sensitive isotopic parameters such as $\Delta^{17}O$.

## 3. Description of the New High-Resolution Continuous Melter system for Sea Ice

### 3.1. Design Considerations

We have designed a melter system capable of processing a full range of ice core types, from clean glacial ice to sediment-laden sea ice. Key differences in density, sediment load, brine channel presence, diameter, fracture frequency, and refreezing behavior drove our selection of flow rates, chemically inert materials, melting temperatures, and tubing diameter.

While our melter system could handle a variety of ices, our current setup is optimized specifically for sea ice cores, which present unique challenges due to relatively high sediment loads and brine channel networks that impact density and porosity. To address these challenges, we incorporated three crucial design features: (i) laser distance measurement for precise melt rate control and consistent sampling resolution independent of density variations (modified from Dallmayr et al., 2016). In addition, electronic controls ensure discrete sampling at predetermined depth intervals rather than volume-based collection, helping in cores with highly variable densities, such as sea ice cores with brine channels; (ii) multi-stage inline filtration to manage high particulate loads; (iii) a circular melt head engineered for whole sea ice core processing, eliminating the need for sectioning and maximizing sample recovery from the inner (uncontaminated) and outer (potentially contaminated) meltwater channels. The complete system comprises four operational stages (Fig. 2), detailed below.

https://doi.org/10.5194/egusphere-2026-4356
Preprint. Discussion started: 18 August 2026


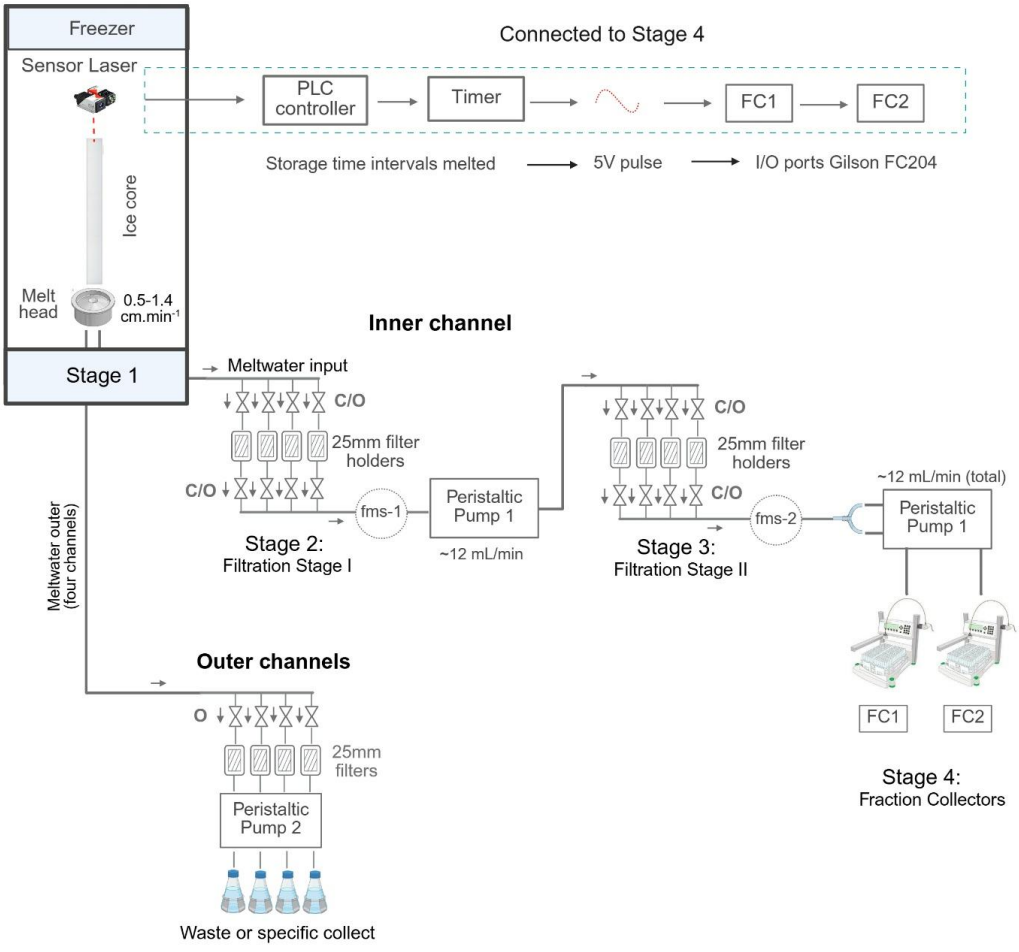


**Figure 2. Schematic of our CMDS with two-stage sequential filtration for sea ice processing. Ice cores melt in Stage 1 (freezer with sensor laser and melt head). Meltwater from the inner channel flows through Stage 2 (Filtration Stage I) and Stage 3 (Filtration Stage II) with switching valves (SV) and 25 mm filter holders (configured for single-line operation with four alternative channels available), driven by Peristaltic Pump 1 (Masterflex Ismatec multichannel pump Reglo ICC. Valves are designated as C/O (closed/open) depending on the active line configuration. Stage 4 contains fraction collectors (FC1, FC2) for sample collection. Flow monitoring sensors (fms-1, fms-2) track flow rates. The dashed box shows freezer connection to Stage 4 via PLC controller and timer (details in Supplementary Materials). Outer channels meltwater flow is drawn by Peristaltic Pump 2 (Gilson MiniPuls 3) for parallel filtration, configured to remain permanently open (O) during the analytical run.**

### Stage 1: Melt Head, Freezer, and Temperature Control (Housed at -15ºC)

The circular melt head is made from aluminum with a 2.54 µm nickel interlayer and a 2.54 µm gold coating to ensure high thermal conductivity and chemical inertness (Fig. 3). Our circular melt head design accommodates entire cores up to 4 inches (~10 cm) in diameter (modified from Kjær et al., 2021). The melt head also has 5 different water channels: one central channel for the inner core and four outer channels for the outer core meltwater (Fig. 3). The

https://doi.org/10.5194/egusphere-2026-4356
Preprint. Discussion started: 18 August 2026


inner channel, located at the base of a 50 mm diameter inner cone, is dedicated to collecting the least contaminated inner ice. This channel also includes space for an exchangeable custom gold-coated mesh filter (2mm pore space) for initial large particulate removal. Both the inner and outer channels have 4.76mm holes connected to 2.4mm inner-diameter PTFE tubing. To avoid the potential risk of lateral mixing at the melt head interface we opted for a concentric shoulder (see Fig. 3) designed to separate flow paths for the central zone and the outer ring (based on Kjaer et al., 2021). This physically separates the inner and outer channels to mitigate meltwater interaction by lateral spreading.

Temperature regulation was achieved using four custom 150W cartridge heaters (Nordic Sensors) installed through threaded connectors, with monitoring using a Type-K thermocouple (Nordic Sensors) and control through a commercial Proportional–Integral–Derivative (PID) controller (Twidec - Model MV100-B10). Operating temperatures range from 10–15°C resulting in melt rates of 0.5 to 1.4 cm $min^{-1}$.

https://doi.org/10.5194/egusphere-2026-4356
Preprint. Discussion started: 18 August 2026


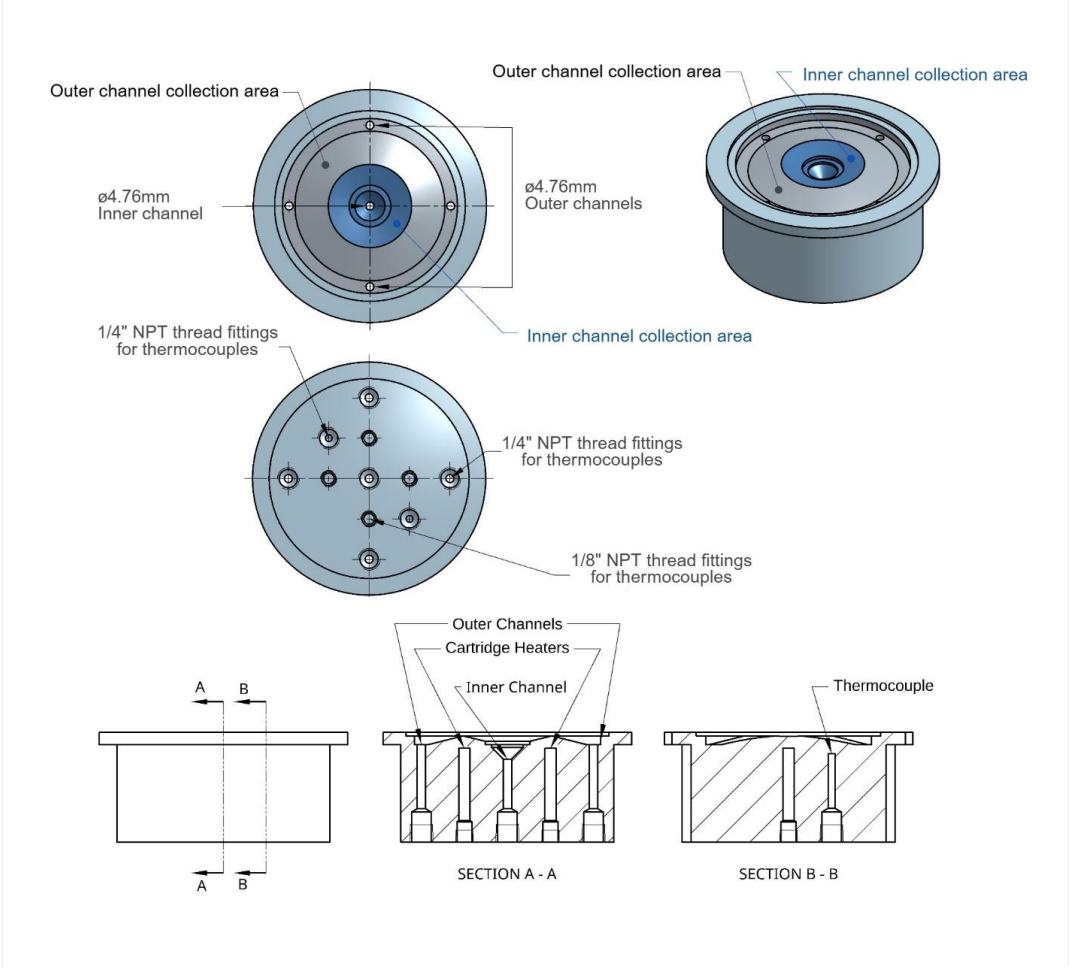


**Figure 3. Melt head design schematic. The cross-section indicates the cartridges heaters and thermocouple position in the melt head.**

### Stages 2 & 3: Multi-stage Inline Filtration

Due to elevated sediment concentrations in sea ice cores, we required meltwater filtration to prevent particle accumulation within the tubing and detector contamination. Previous studies have emphasized the importance of in-line filtration for sediment laden ice (Osterberg et al., 2006). We included two multi-stage filtration stages within our flow system (see Fig. 2) using 25mm polypropylene Swinnex filter holders (Millipore) in series on both the inner and outer flow channels. This configuration allows flexible use of exchangeable membranes with varying pore sizes for targeted particle size-fractionation or comprehensive filtration of all entrained particles within the meltwater.

To maintain continuous operation, parallel filtration lines were installed at both stages, connected via custom SV manifolds (see stages 2 and 3) that allow filter membrane exchange without interrupting melt flow. Keyence FD-XS

https://doi.org/10.5194/egusphere-2026-4356
Preprint. Discussion started: 18 August 2026


series FMS were clamped directly to the tubing downstream of each filtration stage. FMS monitors the flow rate in real time, with a 20–30% reduction from the system flow rate (~12 mL min$^{-1}$) serving as an indicator of membrane saturation. This decrease in flow rate informs the operator to manually switch between filtration lines and facilitates the replacement of membranes loaded with particles, resulting in a minor disruption to the flow. Filtration stage 1 uses a pore size ≥ 1µm, while filtration stage 2 can achieve membranes ≥0.45 µm. In our system, a debubbler was not required because the FMS is designed to tolerate bubbles in the flow path while maintaining accurate flow measurements. In addition, the collection occurs in discrete fractions rather than being directed to downstream instrumentation, eliminating the need for bubble removal.

**Stage 4: Electronically Automated Sampling and Resolution Control**

Sampling resolution is controlled by a laser distance sensor (Dimetix D-Series, model DAE-10-050) with ±1.0 mm accuracy and ±0.3 mm repeatability, capable of operating at temperatures down to –40°C. The sensor continuously monitors the distance between the melt head and the top of the ice core. When the predetermined melt depth is reached, the laser triggers a pulse to a Programmable Logic Controller (PLC).

The PLC output triggers a custom Arduino-based timer controller, which in turn sends a signal (0-5Vdc) to switch vials in the Gilson FC204 fraction collector (FC). The timer controller is attached downstream of the PLC to account for meltwater movement through the tubing between the melt head (where the laser pulse is generated) and the fraction collector (where the vial switch occurs). This electronic configuration greatly reduces lag-time delay between melting and sample collection, as long as flow is steady over time.

The timer continuously records and stores the time intervals between successive laser pulses. The initial vial switch is manually triggered through a touchscreen interface; the controller uses the recorded pulse intervals to automatically synchronize subsequent vial switches. This approach preserves temporal resolution by adapting shifts in melt rate caused by heterogeneous ice properties, such as variable brine channel density or sediment concentration. Detailed electronic settings connecting stages 1-4 are described in the Supplementary Material.

## 4. Results – Melter System Validation Tests

To ensure that our melter system could handle sensitive and complex ice core samples, a series of validation experiments were performed. We conducted four different tests prior to using the system for real sea ice to address changes in density (section 4.1), potential mixing (4.2), contamination (section 4.3), and filtration capability (section 4.4). For these validation tests, our melt head temperature was set to 10°C and pump rate to 6 mL min$^{-1}$ with melt rates ranging from ~0.5–0.8 cm min$^{-1}$.

### 4.1. Test 1 – Density variability

Test 1 (T1 – Density) evaluated the volume collected per vial as a function of core density and depth resolution. This experiment was designed to assess the range of high–depth–resolution sampling for varying sea ice densities between 0.7–0.9 g cm$^{-3}$ (Timco and Frederking, 1996). For T1, we prepared a suite of artificial cylindrical

https://doi.org/10.5194/egusphere-2026-4356
Preprint. Discussion started: 18 August 2026


cores with densities spanning this range and melted them at 0.5 and 1.0 cm resolution. The artificial ice cores were created in the laboratory by freezing deionized (DI) water into solid blocks of ice, breaking the ice into smaller ice fragments (typically centimetric to sub–centimetric), and transferring them into a cylindrical mold. The fragments were subsequently refrozen in the mold, yielding low-density, partially consolidated ice cores with interconnected pore spaces. Densities were determined by averaging mass, height, and diameter measurements with precision scales and calibrated instruments. Because density is not homogenous throughout each artificial ice core some variability in volume is expected.

We found that at a resolution of 0.5cm, collected volumes ranged from 2.67 to 5.71 mL (per vial) with standard deviations between 9.8% and 12% (Fig. 4A). At 1 cm resolution, volumes ranged from 6.75 to 12.30 mL (per vial) with standard deviations between 9.93% to 11.47% (Fig. 4B). Given the volumes obtained at different resolutions, this test demonstrated that our melter system is suitable for most analytical procedures performed on low to high density ice cores at a minimum resolution of 0.5 cm.

T1 also demonstrated that the system responds linearly to ice density at both of the tested depth resolutions (0.5cm, 1.0cm). The coefficient of determination for the linear regression between density and all individual volume measurements shows a fit ($R^2 = 0.63$; $p < 0.001$) at 0.5 cm and $R^2 = 0.51$ ($p < 0.001$) at 1.0 cm depth resolution. The remaining scatter is modest and consistent with vertical heterogeneity in porosity rather than with instrumental noise. This pattern confirms that the melter tracks density-driven variations in melt yield in a stable and predictable way across the range of densities relevant for sea ice cores.

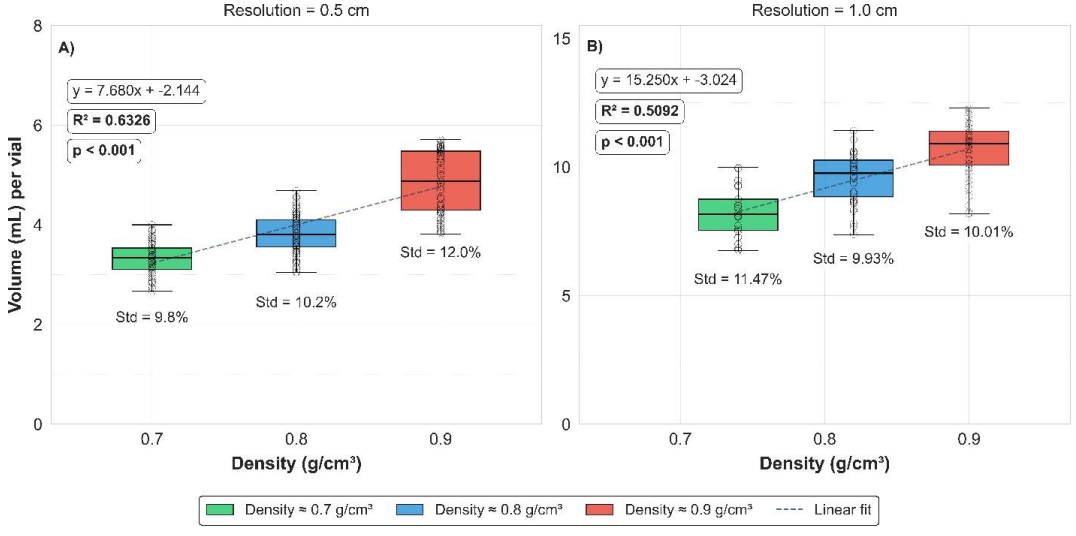


**Figure 4. The volume test results (T1) response to ice density across measurement resolutions. Figures A) and B) show meltwater volume distributions across three estimated densities (~0.7, ~0.8, ~0.9 g cm⁻³) using 0.5 and 1.0 cm sampling resolutions respectively, with standard deviations annotated. Values for linear density–volume relationships for both 0.5cm and 1.0cm sampling resolution were retrieved from regression equations and 95% confidence intervals. Raw data are presented in the supplementary materials.**

https://doi.org/10.5194/egusphere-2026-4356
Preprint. Discussion started: 18 August 2026


### 4.2. Test 2 – Mixing

To replicate the natural saline interlayer variability observed in sea ice cores, we designed Test 2 (T2 – Mixing) to evaluate potential mixing between adjacent layers. Circular ice discs with heights of 15–20 mm were prepared using two contrasting compositions: (i) high-salinity layers ("salty discs") produced from deionized (DI) water with 0.60M NaCl to simulate seawater conditions (~35 practical salinity units, PSU), and (ii) low-salinity layers made from DI water only (~0 PSU). Four DI discs and three salty discs were alternately stacked to construct an artificially stratified core (Fig. 5A). The stack was then melted while collecting samples at high-resolution depth intervals of 5.0 mm (Fig. 5B), and conductivity was measured for each fraction to quantify cross-layer mixing.

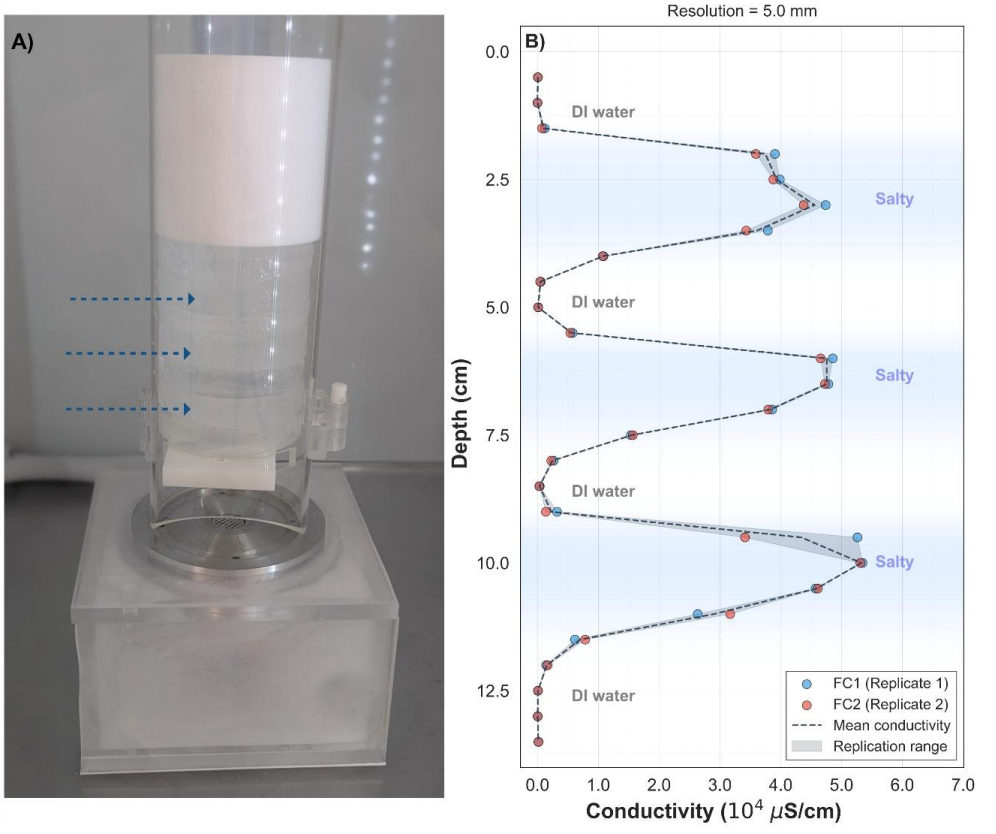


**Figure 5. Conductivity profiles in artificially stratified ice. Alternating layers of deionized water (DI water) and NaCl-enriched ice (Salty) were melted using aluminum melt head. (A) Interlayered discs. Blue arrow indicates the salty discs (B) 5.0 mm resolution intervals. FC1 and FC2 represent replicate conductivity measurements. transitions between layers indicate preservation of salinity boundaries despite vertical resolution limitations. More details in supplementary material.**

Given the presence of high–salinity in sea ice cores, cross–contamination between adjacent low– and high-salinity regions can occur during melting, potentially affecting signal resolution. T2 preliminary results demonstrate reproducible conductivity transitions between adjacent layers, confirming that our melter system preserves high and low salinity signals during melting. However, because vial switching depends on laser-detected core distance rather

https://doi.org/10.5194/egusphere-2026-4356
Preprint. Discussion started: 18 August 2026


than layer–specific characteristics, variable disc heights limit quantification of interlayer mixing and carryover evaluation. Precise contamination assessment requires methodological refinement to decouple physical mixing from sampling artifacts.

### 4.3. Test 3 – Contamination

Test 3 (T3 – Contamination) addressed carryover and contamination within the system. Both nutrient and trace metal contamination were tested. For nutrients, the USGS round-robin N-160 reference standard (nitrate+nitrite, orthophosphate and ammonium) was used, with typical spike concentrations on the order of ~1500 ppb for nitrate+nitrite, ~100 ppb for orthophosphate and ~500 ppb for ammonium, comparable to the upper range of macronutrient enrichments reported (Cozzi, 2008). In this test, one sample (10ml) of this standard was pipetted into the system followed by three samples of DI water (10ml each, 30ml total; Fig. 6). The collected samples were analyzed by Skalar SAN$^{++}$ Continuous Flow Nutrient Analyzer. In parallel, we pipetted the same standard volumes directly into pre-cleaned vials, bypassing the melter and flow path, to provide an external reference result and to isolate potential errors associated with standard preparation from system-induced carryover.

For trace metals, the Inorganic Ventures ICPMS-71A reference standard (23 elements analyzed) was used. In this test, we created a diluted solution of the reference for all elements (~100 ppb) and acidified it with 2% $HNO_3$. Again, one sample (10ml) of our solution was injected into our system followed by four samples of DI water (10ml each, 30ml total; Fig. 7). The collected samples were run on an ICP-OES (Perkin Elmer Optima 7300 DV) in the Trace Element Research Laboratory (TERL) at The Ohio State University. The elevated standards were selected to maximize analytical signal and to provide a conservative assessment of carryover under large concentration steps, rather than to reproduce ambient trace-metal concentrations, which generally occurs in the low-ppb to nanomolar range in natural ice. Between tests, we modified cleaning procedures previously outlined by GEOTRACES (Cutter et al., 2017). In brief the inner channel was rinsed with 0.1% Citranox for 1 h followed by deionized water for an additional hour. In contrast, the outer channels carrying excess meltwater could be cleaned with deionized water only.

For both contamination tests, carryover was quantified by first correcting all measurements for the analytical baseline and then expressing the residual signal in each post-peak fraction as a percentage of the corresponding peak concentration. For a given fraction $i$, the baseline-corrected residual signal $R_i$ was obtained as $R_i = S_i - B$, where $S_i$ is the raw signal in fraction $i$ and $B$ is the mean baseline signal estimated from pre-pulse blanks. The effective peak concentration $P$ was calculated as $P = S_{\text{peak}} - B$, with $S_{\text{peak}}$ denoting the raw signal at the peak maximum. The carryover for fraction $i$ was then defined as $\text{Carryover}_i(\%) = (R_i/P) \times 100$, thereby reporting memory effects as the fraction of the original peak signal that persists into subsequent samples after removal of background contributions.

In nutrient analysis, carryover tests showed low memory across all analytes (see supplementary material), with residual signals confined mainly to the first one to three fractions following each peak. For Nitrate + Nitrite, the maximum carryover in the first post-peak sample ranged from ~5–9% of the concentration peak, while the integrated contribution of all post-peak fractions remains below ~10% for each pulse. Ammonia exhibits a very similar behavior, with

https://doi.org/10.5194/egusphere-2026-4356
Preprint. Discussion started: 18 August 2026


peak-to-peak carryover maxima of ~5– 7% and total residuals on the order ~6–10% of the original peak signal. Phosphate shows the lowest memory overall, with maximum carryover typically between 3 and 7% and integrated post-peak contributions that were generally below 9% and, in some cases, statistically indistinguishable from the baseline when positive and negative residuals are considered together. These results demonstrate that the melter and analytical setup introduced little to no nutrient contamination. Further, the peak concentrations measured after passing through the system closely match the original standard concentrations, differing by only a few percent. This indicates that the system preserved the concentration peak with minimal dilution or loss for all nutrients performed during the test.

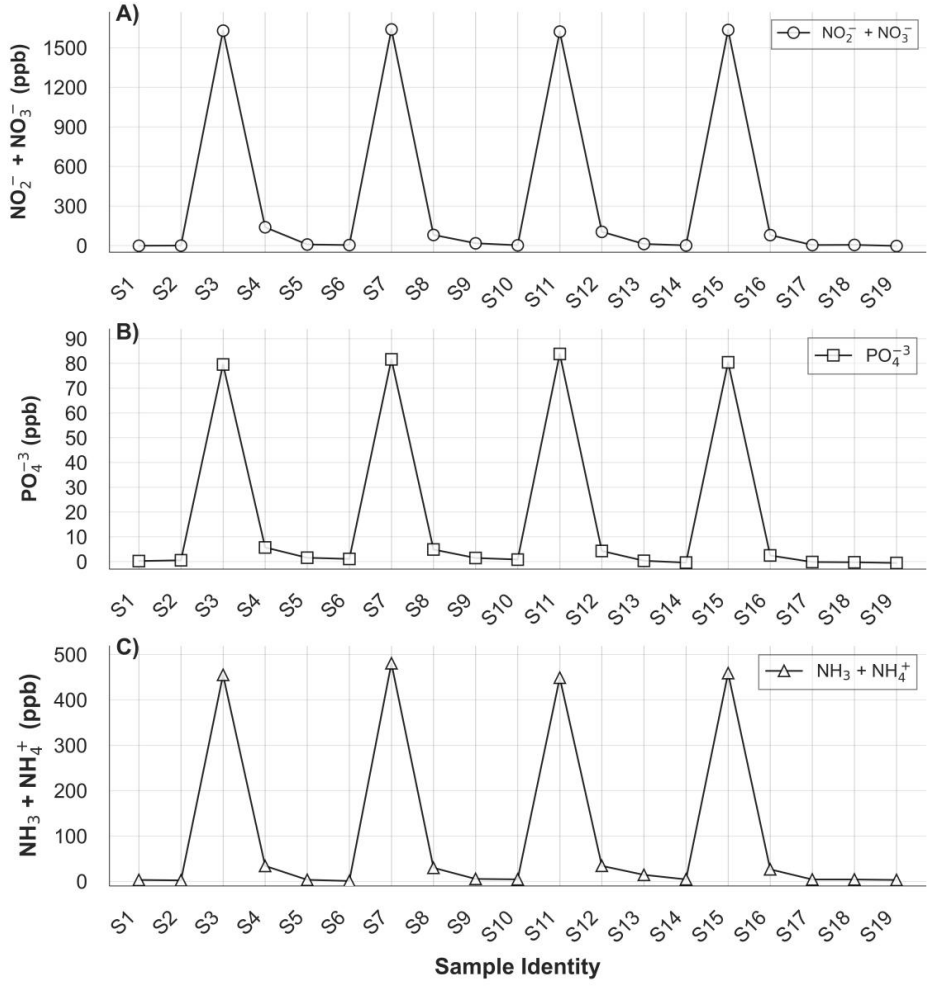


**Figure 6. Validation test T3 to assess mixing behaviour of the nutrients nitrate+nitrite (NOx), orthophosphate ($PO_4^{3-}$) and ammonia ($NH_4^+$). Alternating nutrient standard pulses (S3, S7, S11, S15) were introduced among DDI water blanks. Peak concentrations are preserved, indicating contamination-free nutrient profiles in panels a, b and c. Estimated LOD/LOQ**

https://doi.org/10.5194/egusphere-2026-4356
Preprint. Discussion started: 18 August 2026


**values were 2.37/7.18 ppb for NOx, 2.79/8.46 ppb for $NH_4^+$, and 0.57/1.74 ppb for $PO_4^{3-}$. Full data and LOD/LOQ calculations are provided in the supplementary materials.**

For metals, our goal was to assess sample carryover behavior across twelve key elements, ordered to reflect our analytical workflow: major cations (Ca, K, Na, Mg), bioactive transition metals and micronutrients (Fe, Mn, Cu, Zn, Co), and less abundant trace elements (Cr, Th, V). The results reveal a consistently low carryover pattern, with residual contamination (<10%) typically confined to one or two fractions immediately following each concentration peak (S4, S10, S15, S20; Fig. 7).

In this test, Ca and Zn exhibited carryover signatures post-peak, with residuals reaching approximately 8–10% of the original peak magnitude in the first fraction. Meanwhile, the carryover values decline rapidly in subsequent samples. Most elements, including K, Na, Mg, and the transition metals Fe, Mn, Cu, V, Cr, and Co, showed moderate post-peak carryover (ranging from 2 to 6%). Notably, Th, V, Cr, and Co exhibited the lowest carryover values, consistently remaining below 5% in the immediate post-peak fraction (see data in the Supplementary Material).

Comparing all data, we see four pulses, with integrated carryover totals (sum of residuals between the peaks) that were mostly below 15%. For the case of the redox-sensitive elements Fe and Mn, which are particularly important to sea ice geochemical analysis, the residuals were below 10%. This rapid observed attenuation (returning to baseline levels by the second or third fraction) and the absence of systematic carryover accumulation confirms that memory effect remains minimal within our CMDS set-up. Nine additional elements (Rb, Sr, Ag, Cd, La, Ce, Pr, Nd, Pb) exhibited similar carryover behavior (low carryover %, Fig. S5, Table S3), and the complete dataset is provided in the supplementary material.

https://doi.org/10.5194/egusphere-2026-4356
Preprint. Discussion started: 18 August 2026


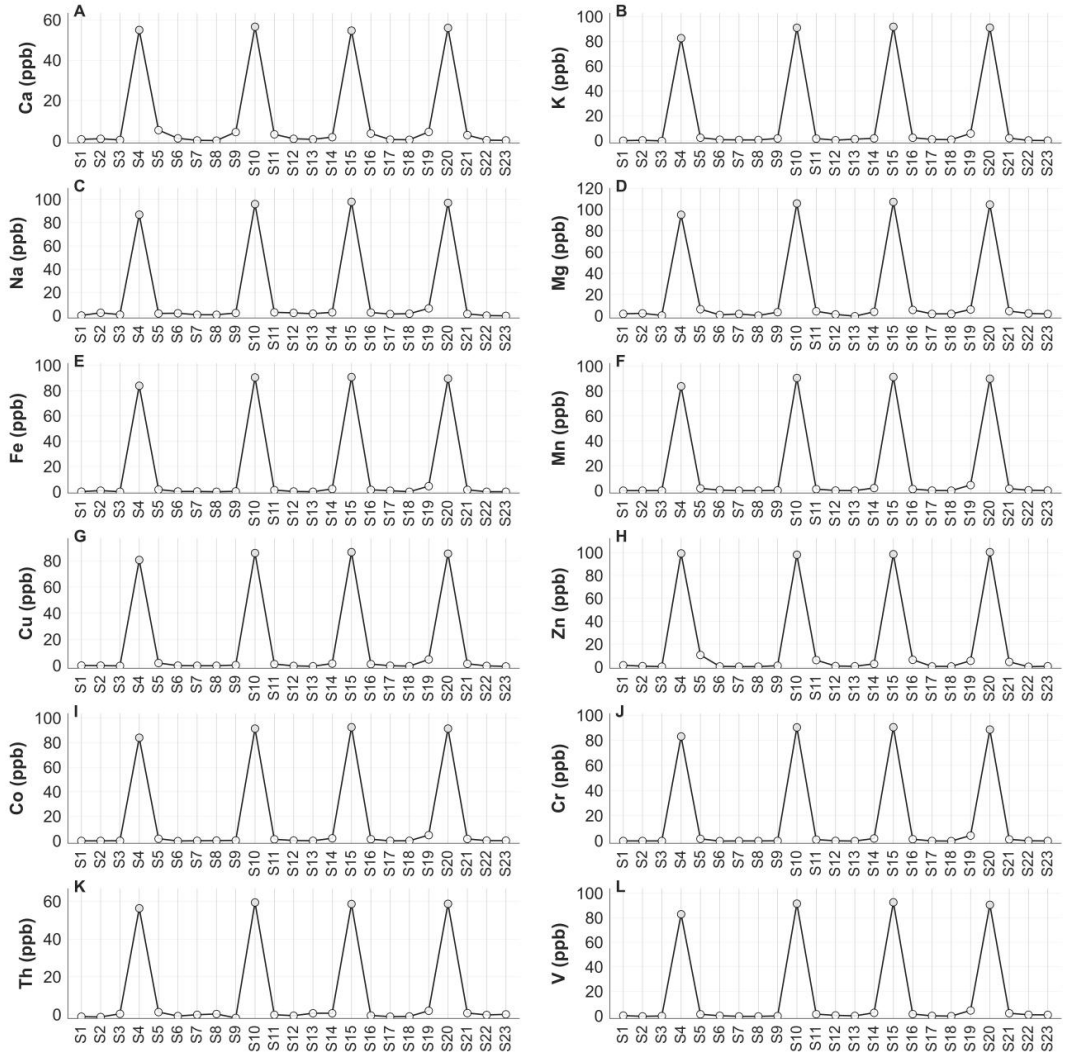


**Figure 7. Trace element concentration profiles across 23 samples for gold-coated melt head. 12 elements (Ca, K, Na, Mg, Fe, Mn, Cu, Zn, Co, Cr, Th, V) measured in ppb from S1 to S23. Samples S4, S10, S15, and S20 represent spiked standards (~80–108 ppb) for most elements, except for Ca (~54.7–56.6 ppb) and Th (~56.3–59.4 ppb), while remaining samples represent deionized water blanks. LOD ranges ~0.07–1.82 ppb and LOQ ranges ~0.24–6.05 ppb. Full data can be accessed in supplementary materials.**

### 4.4. Test 4 - Filtration

Test 4 (T4 – Filtration) assessed particulate recovery by the filtration system using circular ice discs containing 148 mL of DI water and 50 mg of pre-sieved dust in a circular mold of 3.73 inches diameter. A locally-collected dust sample (Columbus-OH, U.S.; 1–106 µm) was chosen to span the grain sizes expected in sediment-laden sea ice cores (as observed in previous studies, e.g., Nürnberg et al., 1994; Reimnitz et al., 1998) and to test retention on a 1 µm

https://doi.org/10.5194/egusphere-2026-4356
Preprint. Discussion started: 18 August 2026


pore-size polycarbonate membrane mounted in the first filtration stage. Materials from both inner and outer channels were collected on these membranes. Between each experiment all connectors, filter holders, and lines were flushed with DI water to release any trapped sediment and minimize background contamination.

Across five replicates, the system achieved a mean recovery exceeding 80% (Fig. 8), with most of the solid mass retained on the membrane surface within the targeted size range. We account for the remaining deficit with particles becoming trapped in connections and other small dead volumes along the flow path, as well as potential chemical weathering and salt dissolution that may be occurring, rather than with systematic loss through the filter itself. From a practical standpoint, this level of recovery demonstrates that the filtration stage is effective for capturing the particulate load relevant to most sea ice applications.

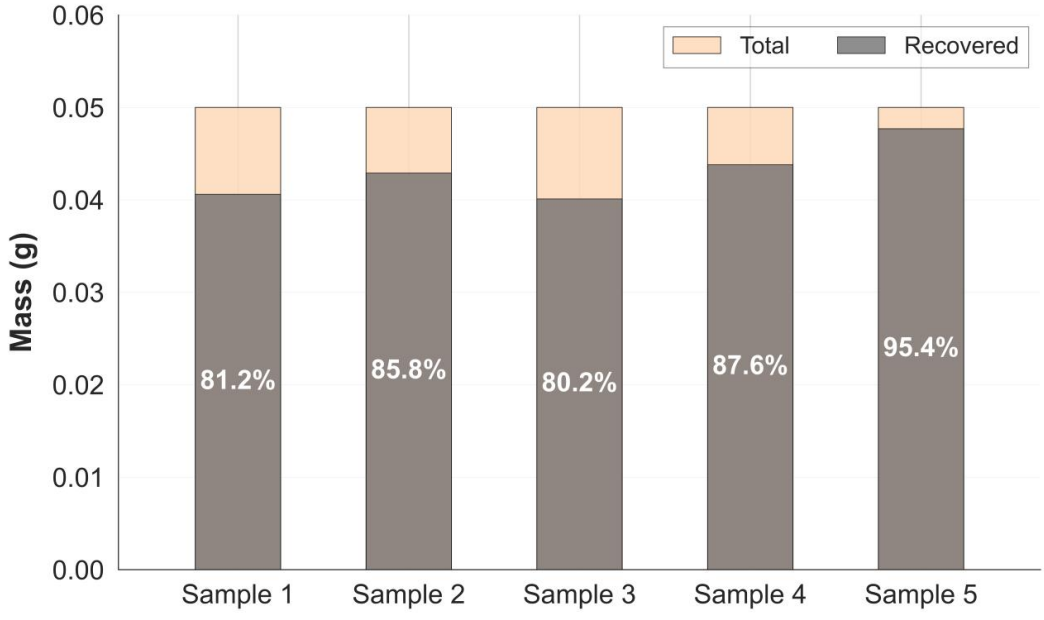


**Figure 8. Sediment recovery analysis from melter system. Five replicate samples (3.73 inches diameter, 18 mm height discs) with fixed input mass (0.050 g, conc. ~337.83 mg/L) were processed to evaluate solid-phase capture efficiency. Recovered mass ranges from 0.0401 to 0.0477 g, yielding recovery rates between 80.2% and 95.4%, with a mean recovery of 86%. Percentages displayed within bars indicate recovery efficiency per sample, demonstrating consistent sediment capture across replicates with acceptable variability (±6.1%).**

## 5. Discussion

Previous high-resolution continuous melter systems have been primarily developed for relatively pure ice cores with low sediment loads and homogenous densities from polar and alpine regions (Bigler et al., 2011; McConnell et al., 2002; Osterberg et al., 2006; Röthlisberger et al., 2000). Those melter systems may face significant challenges when

https://doi.org/10.5194/egusphere-2026-4356
Preprint. Discussion started: 18 August 2026


applied to complex, high-impurity matrices such as sea ice cores. In contrast, our *ICARUS* system is designed to preserve sample integrity across a wide range of physical and chemical conditions.

### 5.1. Main sea ice core process challenges

#### 5.1.1. Addressing Design Challenges from Sea Ice Physical Properties

One important feature of the artificial ice cores analyzed in this study, compared with ice cores processed in other systems (e.g. the CMDS system), was their density variability. Sea ice core densities are generally heterogenous throughout and can vary significantly over short vertical distances (from ~0.72 to ~0.93 g $cm^{-3}$) due to the presence of brine channels and variations in porosity, temperature, and sediment load (Hutchings et al., 2015; Timco and Frederking, 1996). This can directly affect ice core density at centimeter and sub-centimeter scales (Hutchings et al., 2015). In contrast, freshwater ice cores generally comprise firn and layers of snow densification based on high accumulation and low temperature over time, which leads to density profiles that are often less structurally complex (Thomas et al., 2021). The increased structural complexity in sea ice cores leads to a significant challenge that requires a variable melt-rate regime to account for cores with lower or more heterogeneous density that can melt more rapidly or non-uniformly, requiring careful control of melt conditions.

Although other CMDS systems have used drop counting (e.g. 100 drops per sample) to represent depth intervals, the structural heterogeneity found in sea ice implies that equal meltwater volumes do not necessarily correspond to equal ice-core depth intervals, making fixed drop counts a less reliable proxy for depth in this material. Therefore, in our experiments we measured our cores based on fixed depth intervals (e.g., 1 cm) and tracked distance down-core with a laser height sensor. This strategy minimizes bias from local density and porosity variations.

In our experiments, we intentionally introduced high and low porosity layers during laboratory ice preparation to reproduce structural characteristics typical of different ice types (ranging from ~0.7-0.9 g/$cm^3$). Our findings indicated that our system has the advantage of collecting meltwater at a set resolution rather than presetting a vial drop count. This allows our system to process all ice types even if porosity within the same core is variable. This is important because variable melt rates can distort sample resolution and introduce biases in concentration results (Osterberg et al., 2006). Our findings indicate that the *ICARUS* system has the advantage of collecting meltwater at a set resolution rather than presetting a vial drop count, allowing for processing of all ice types.

#### 5.1.2. Signal Preservation Across Boundaries

Other factors that we needed to consider were complex matrices driven by salinity. Sea ice cores' bulk salinity ranges from 0.4 to 5 PSU, and in areas containing brine channels salinity can exceed 100 PSU (Dieckmann and Hellmer, 2009; Wang et al., 2020). We were interested in preserving these high brine signals, as they are of scientific importance to understanding brine migration (Golden et al., 1998), biological hotspots, and solute movement (Petrich and Eicken, 2017).

To evaluate changes in salinity, we assessed the system's ability to resolve and accurately record conductivity transitions between high-salinity brine (35 PSU, representative of seawater) and low-salinity (0 PSU) sea ice

https://doi.org/10.5194/egusphere-2026-4356
Preprint. Discussion started: 18 August 2026


conditions (Fig. 5). Our system exhibited effective preservation in salinity stratigraphy maintaining clear contrasts between low-salinity layers with conductivities on the order of $10^1$ µS/cm and brine-enriched layers with conductivities on the order of $10^4$ µS/cm (note: 50,000 µS/cm NaCl in DI = ~32 to 35 PSU). These results indicate that the system can reliably identify brine-enriched layers in sea ice cores, with salinity variability in our experiment driven mostly by disc height differences (see section 4.2.). Further, our raw conductivity data indicated limited signal attenuation and dispersion, confirming a reassuringly low extent of interlayer mixing. These tests indicate that our system can accomplish the identification and quantification of brine rich layers in sea ice cores under high resolution performance, extending our capabilities to study across the physical complexities that are routinely observed in sea ice.

#### 5.1.3. Carryover, Memory Effects, and Geochemistry

The continuous melting and delivery of samples at centimeter and sub-centimeter resolution to fraction collectors and instruments is of importance for all ice types, including polar and mid-latitude ice cores (Bigler et al., 2011; Kaufmann et al., 2008; Osterberg et al., 2006). However, carryover and memory effects can pose challenges for the high-resolution analysis of trace metals, nutrients, and organic matter since they can distort vertical gradients and thin stratigraphic horizons. In sea ice, geochemical stratification is particularly important because solute distributions can provide important information on ocean-ice biogeochemical coupling (e.g., the supply of nutrients and micronutrients) that may increase primary production and the development of biological hotspots (Lannuzel et al., 2016; Miller et al., 2015; Tovar-Sánchez et al., 2010; Vancoppenolle et al., 2013). Past studies have indicated that dissolved trace metals (e.g., Fe, Mn, Cd and Cu) in Arctic and Antarctic sea ice and brines typically range from sub-nanomolar to tens of nanomolar concentrations (e.g. Duprat et al., 2020; Evans and Nishioka, 2019; Lannuzel et al., 2011; Wang et al., 2014). Vertical gradients of a few nmol $L^{-1}$ along centimetric intervals are required to resolve any variability of micronutrients in sea ice. However, it is difficult to measure the magnitude of such small vertical micronutrient gradients within high-resolution sea ice using presently available processing techniques: our new system has been designed to overcome that limitation.

In our experiments, we quantified carryover because memory effects can affect geochemical results by obscuring thin layers in ice, suppressing peaks, and altering gradients. Our findings show that the first post-peak sample consistently measured less than 10% of peak concentrations for nutrients and trace elements, with carryover dropping to less than 1% in all subsequent samples (Figs. 6 and 7). For additional trace-metal elements (e.g. Ag, Cd, REE), residual concentrations in post-pulse samples were typically 0–2 % of peak values (see supplementary material). Further, the limits of detection for key trace metals measured by ICP-OES were on the order of 0.1–2 ppb (1–30 nmol $L^{-1}$, depending on the element) and, hence, comparable to or below the lower range of micronutrient concentrations previously reported in sea ice (Duprat et al., 2020; Evans and Nishioka, 2019; Lannuzel et al., 2011; Wang et al., 2014). Importantly, our validation tests show that any positive bias in the first post-peak sample is limited to ≤10%, whereas subsequent samples are effectively unaffected; this suggests that minimal carryover is to be anticipated during natural archive runs. Thus, our system can resolve nanomolar-scale variations in trace-metal gradients at high spatial

https://doi.org/10.5194/egusphere-2026-4356
Preprint. Discussion started: 18 August 2026


resolution, while consistent low memory across all elements minimizes systematic bias and ensures that thin geochemical horizons can be resolved within an ice-core.

Previous ice core melter systems have reported minimal sample cross-contamination and signal smoothing due to dispersion in the melt head and flow path, particularly for sticky analytes and large concentration steps (Jones et al., 2017; Kaufmann et al., 2008; McConnell et al., 2002; Osterberg et al., 2006). Our configuration indicates similar memory effects at the sub-percent carryover scale for most elements (see Figs. 6 and 7). The similar use of chemically inert flow path materials in our system (i.e. PTFE tubing, gold-coated melt head) contributed to favorable performance and aligns with the best requirements for ultra-trace element analysis highlighted in pioneering works (Bigler et al., 2011; Knüsel et al., 2003; McConnell et al., 2002; Osterberg et al., 2006; Röthlisberger et al., 2000). By addressing these challenges, we can confidently resolve small geochemical gradients in sea ice cores and make inferences for nutrients and trace metal inputs from sea ice to the ocean.

#### 5.1.4. Inline Particulate Recovery

This new system can simultaneously collect both dissolved and solid phases from the same melt stream. Some ice types, such as sea ice and some sediment-rich alpine ice, can carry high particle loads including mineral dust, volcanic ash, microorganisms, and organic matter. These particle loads can record atmospheric deposition, transport pathways, and sources of sediments that may be linked to biological productivity, among other environmental signals (Corkill et al., 2025; Darby et al., 2011; Reimnitz et al., 1993). This capability allows direct coupling of geochemical and physical signals within the same depth interval, preserving co-located signals from dissolved ions, particulates, and organic matter that would otherwise be partly lost or decoupled through separate processing. It also enables targeted studies, for example investigations of iron-bearing mineral dust associated with dissolved iron and organic carbon in sea ice layers or joint analysis of volcanic ash shards and acidity peaks. Further, our multi-stage filtration system permits separation of various grain size fractions, allowing for targeted investigations of aerosol deposition, sea ice biogeochemistry, and sediment transport processes.

The solid-phase capture in the system represents an advancement in discrete sampling systems, which previously focused, primarily, on dissolved or total elemental concentrations and provided only limited control over particulate recovery (Osterberg et al., 2006). The alternate lines in filtration stages 1 and 2 also allow the capture of specific layer depths without interruptions to the continuous melting process (Fig. 2). Finally, exchangeable membrane capabilities allow us to capture specific range-size targets in meltwater (>0.45um) to answer different scientific questions. Overall, the inclusion of in line filtration unlocks the potential to address research questions about sea ice, beyond current capabilities available.

### 5.2. Melt Rate Considerations

Our system operates at lower melt rates (see Table 1) to address signal dispersion and depth resolution challenges with a maximum pump rate of 15mL.min$^{-1}$. This can achieve an estimated melt rate of ~1.0–1.4 cm.min$^{-1}$ depending on the density and melt head temperature. This is important to counter prior observations by Breton et al. (2012) that low density core sections, such as firn, can present shifted chemistry peaks resulting in the reduction of depth resolution.

https://doi.org/10.5194/egusphere-2026-4356
Preprint. Discussion started: 18 August 2026


In CFA and CMDS configurations, melt rates have been constrained, generally, by the flow requirements of coupled instruments and the length of ice cores, respectively. For example, some CMDS systems are optimized to operate at 1.5–3 cm $min^{-1}$ (Osterberg et al., 2006) to handle multi–hundred–meter to kilometer–scale ice-sheet records, where rapid throughput is essential. In contrast, our system is optimized to operate at lower melt rates to prioritize processing shorter, impurity-rich cores. Here, stratigraphy preservation, minimal contamination, and depth-control at the centimeter–scale are the primary advances that our melt rate supports.

### 5.3. Recommendations

Despite a strong overall performance, our gold coated melt head did present a few limitations for some specific analytes. For example, in this study we excluded Aluminum (Al) and Nickel (Ni) from the T3 validation test results because carryover in the first post-peak fraction exceeded 20%. In all tests, both elements yielded highly variable results and suffered from continuous contamination. We hypothesize that this elevated carryover may reflect small layering imperfections within the (Au/Ni/Al) melt head suggesting that it may not be ideal for Al and Ni quantification. The assembly includes an Al body plated with Ni and an overlaying gold coating, likely promoting adsorption, retention, and/or delayed release of these metals during sample melting. To address this, we found that having exchangeable melt heads with different coating materials can be important to allow for flexibility in ice core analysis. For example, we would recommend a fluorinated ethylene propylene (FEP) coated melt head if Al and Ni are a priority. Preliminary results from experimentation with an FEP melt head (see supplementary files for trace metal and cation data; Fig. S6, Table S4) show lower contamination (5–15%) for Al and Ni. In other cases, materials like aluminum may be used for analyses such as bulk oxygen isotope analysis or organic geochemistry, each of which require less rigorous inorganic trace element and isotopes cleanliness.

Beyond the choice of materials for future melt head assembly, we would also advise the processing of melt cores from significantly different salinity regimes (such as brine-rich sea ice, polar ice, and tropical glacier ice) in separate runs. Additionally, cores with high particulate loads (for example volcanic ash layers) will need extra care during stages 2 and 3 of the melting procedure (Fig. 2). In such cases, close attention to the flow sensors will be needed to keep flow rates stable, to maintain the target depth resolution, and to limit excessive mixing. Furthermore, the cadence for replacement of the inner and outer tubing channel should be determined from the levels of contamination observed in blank runs. In general, the inner tubing should be replaced more frequently than outer.

## 6. Conclusions

Our new validated high-resolution continuous melter system designed specifically for sediment-laden ice core applications combines discrete sampling with integrated multi-stage filtration, real-time meltwater flow rate monitoring, and electronic depth-resolution control. These combined capabilities address the primary analytical challenges to the investigation of sea ice and other high-impurity ice cores, representing an advance over existing continuous melter systems and discrete-sampling approaches. Significant features of this system include: (i) a full-core melting geometry that eliminates labor-intensive and sample-wasting ice-cutting workflows (similar to Kjær 2021), (ii) laser-based depth control with timing precision to allow for high resolution analyses of discrete samples (Dallmayr et al., 2025), and (iii) adaptive multi-stage filtration enabling both size-fractionation and selective solid

https://doi.org/10.5194/egusphere-2026-4356
Preprint. Discussion started: 18 August 2026


phase capture. These design features improve three documented limitations of previously existing continuous melter systems when used for sea ice core analyses: (i) the loss of particulate-phase geochemical information in CFA-only approaches due insufficient acidification time in high-speed transit systems; (ii) signal attenuation from internal mixing in high-resolution profiling; and (iii) depth resolution control in CMDS systems which, instead, typically offer volume-based resolution.

Our validation experiments, by design, tested the system's capability to handle a suite of critical sea ice core characteristics, confirming reliable sample preservation across the density and salinity regimes of natural ice cores. Overall, our results show that this system can facilitate the acquisition of robust, high-resolution geochemical records with applicability to sea ice and also to multiple other sediment-rich types of ice core that have continued to prove challenging for prior common-use systems. Our new system enables the high-resolution quantitative characterization of micronutrient and trace-metal gradients, brine chemistry, and sediment transport at the centimeter-scale within sea ice. These advances are poised to contribute to novel studies of polar biogeochemical cycles and to enhance the use of sea ice records as analogues for icy ocean worlds through the development of habitability and nutrient transport models that can be applied to extraterrestrial settings.

## Data Availability

All data, supplementary materials, and design files related to the experiments and the continuous melter system are publicly available in the Zenodo repository at DOI: 10.5281/zenodo.21224204. Version 2

Suggested citation: dos Reis, R., Mondragon, D., Magner, N., Vaughn, B., Morris, V., Hand, K., Walker, C., German, C., McConnell, J., Kjaer, H., & Diaz, M. (2026). *A High-Resolution Continuous Melter System for Sea Ice and Sediment-Ladden Ice Applications* (Dataset). Zenodo. https://doi.org/10.5281/zenodo.21224204.

## Author contribution

MAD led the project and the conceptualization of the study. RDR, DM, NM developed methodology, curated the data, performed formal building, analysis and validation tests. NM led all engineering-based activities for this project with oversight from RDR and MAD. RDR and DM wrote the original draft of manuscript. CG, KH, CCW, BV, VM, contributed to conceptualization and project administration. CG, KH, CCW, BV, VM, JM, and HAK contributed with manuscript review and editing. MAD was responsible for funding acquisition and contributed to manuscript review and editing.

## NACompeting interests

The authors declare that they have no competing interests.

## Acknowledgments

The authors thank Ryan Shea of the Ohio State University College of Arts and Sciences, Paul Green of the Byrd Polar and Climate Research Center, Anthony Lutton of the Trace Element Research Laboratory at the Ohio State University, and the Bolz Hall Makerspace at the Ohio State University for their technical and scientific assistance. In addition, we

https://doi.org/10.5194/egusphere-2026-4356
Preprint. Discussion started: 18 August 2026


acknowledge Desert Coating Solutions, Guerrero Plating Technology LLC, and Keyence Sensors for their support and collaboration.

**Financial support**

The authors acknowledge financial support from NASA grants 80NSSC24K0725 and 80NSSC26K0263. HAK acknowledges funding from the European union (101184070 & 101184621) and the Danish Research Foundation (DFF 1131-00007B).

**References**

Abram, N. J., Wolff, E. W., and Curran, M. A. J.: A review of sea ice proxy information from polar ice cores, Quat. Sci. Rev., 79, 168–183, https://doi.org/10.1016/j.quascirev.2013.01.011, 2013.

Arienzo, M. M., McConnell, J. R., Chellman, N., and Kipfstuhl, S.: Method for Correcting Continuous Ice-Core Elemental Measurements for Under-Recovery, Environ. Sci. Technol., 53, 5887–5894, https://doi.org/10.1021/acs.est.9b00199, 2019.

Arrigo, K. R.: Sea Ice Ecosystems, Ann. Rev. Mar. Sci., 6, 439–467, https://doi.org/10.1146/annurev-marine-010213-135103, 2014.

Bacon, S.: Arctic sea ice, ocean, and climate evolution, Science (1979)., 381, 946–947, https://doi.org/10.1126/science.adj8469, 2023.

Barbaro, E., Feltracco, M., Spagnesi, A., Dallo, F., Gabrieli, J., De Blasi, F., Zannoni, D., Cairns, W. R. L., Gambaro, A., and Barbante, C.: Fast Liquid Chromatography Coupled with Tandem Mass Spectrometry for the Analysis of Vanillic and Syringic Acids in Ice Cores, Anal. Chem., 94, 5344–5351, https://doi.org/10.1021/acs.analchem.1c05412, 2022.

Bigler, M., Svensson, A., Kettner, E., Vallelonga, P., Nielsen, M. E., and Steffensen, J. P.: Optimization of High-Resolution Continuous Flow Analysis for Transient Climate Signals in Ice Cores, Environ. Sci. Technol., 45, 4483–4489, https://doi.org/10.1021/es200118j, 2011.

Breton, D. J., Koffman, B. G., Kurbatov, A. V., Kreutz, K. J., and Hamilton, G. S.: Quantifying Signal Dispersion in a Hybrid Ice Core Melting System, Environ. Sci. Technol., 46, 11922–11928, https://doi.org/10.1021/es302041k, 2012.

Cole-Dai, J., Budner, D. M., and Ferris, D. G.: High Speed, High Resolution, and Continuous Chemical Analysis of Ice Cores Using a Melter and Ion Chromatography, Environ. Sci. Technol., 40, 6764–6769, https://doi.org/10.1021/es061188a, 2006.

Corkill, M., Meiners, K. M., Wongpan, P., van der Merwe, P., Creac'h, L., Feig, S., Nelson, T., Smith, A. J. R., Townsend, A. T., Twiname, S., and Lannuzel, D.: Dissolved iron release by sediment and dust particles in Antarctic

https://doi.org/10.5194/egusphere-2026-4356
Preprint. Discussion started: 18 August 2026


seawater greater than glacial flour and sea-ice particles, Mar. Chem., 270, 104509, https://doi.org/10.1016/j.marchem.2025.104509, 2025.

Cozzi, S.: High-resolution trends of nutrients, DOM and nitrogen uptake in the annual sea ice at Terra Nova Bay, Ross Sea, Antarct. Sci., 20, 441–454, https://doi.org/10.1017/S0954102008001247, 2008.

Cutter, G., Casciotti, K., Croot, P., Geibert, W., Geochemistry, M., Heimbürger, L.-E., and Lohan, M.: Sampling and Sample-handling Protocols for GEOTRACES Cruises, 2017.

Dallmayr, R., Goto-Azuma, K., Astrid Kjaer, H., Azuma, N., Takata, M., Schüpbach, S., and Hirabayashi, M.: A High-Resolution Continuous Flow Analysis System for Polar Ice Cores, Bulletin of Glaciological Research, 34, 11–20, https://doi.org/10.5331/bgr.16R03, 2016.

Dallmayr, R., Meyer, H., Gkinis, V., Laepple, T., Behrens, M., Wilhelms, F., and Hörhold, M.: Assessment of continuous flow analysis (CFA) for high-precision profiles of water isotopes in snow cores, Cryosphere, 19, 1067–1083, https://doi.org/10.5194/tc-19-1067-2025, 2025.

Darby, D. A., Myers, W. B., Jakobsson, M., and Rigor, I.: Modern dirty sea ice characteristics and sources: The role of anchor ice, J. Geophys. Res., 116, C09008, https://doi.org/10.1029/2010JC006675, 2011.

Dieckmann, G. S. and Hellmer, H. H.: The Importance of Sea Ice: An Overview, in: Sea Ice, Wiley, 1–22, https://doi.org/10.1002/9781444317145.ch1, 2009.

Duprat, L., Corkill, M., Genovese, C., Townsend, A. T., Moreau, S., Meiners, K. M., and Lannuzel, D.: Nutrient Distribution in East Antarctic Summer Sea Ice: A Potential Iron Contribution From Glacial Basal Melt, J. Geophys. Res. Oceans, 125, https://doi.org/10.1029/2020JC016130, 2020.

Eayrs, C., Li, X., Raphael, M. N., and Holland, D. M.: Rapid decline in Antarctic sea ice in recent years hints at future change, Nat. Geosci., 14, 460–464, https://doi.org/10.1038/s41561-021-00768-3, 2021.

Eicken, H., Gradinger, R., Gaylord, A., Mahoney, A., Rigor, I., and Melling, H.: Sediment transport by sea ice in the Chukchi and Beaufort Seas: Increasing importance due to changing ice conditions?, Deep Sea Research Part II: Topical Studies in Oceanography, 52, 3281–3302, https://doi.org/10.1016/j.dsr2.2005.10.006, 2005.

Emanuelsson, B. D., Baisden, W. T., Bertler, N. A. N., Keller, E. D., and Gkinis, V.: High-resolution continuous-flow analysis setup for water isotopic measurement from ice cores using laser spectroscopy, Atmos. Meas. Tech., 8, 2869–2883, https://doi.org/10.5194/amt-8-2869-2015, 2015.

Erhardt, T., Jensen, C. M., Borovinskaya, O., and Fischer, H.: Single Particle Characterization and Total Elemental Concentration Measurements in Polar Ice Using Continuous Flow Analysis-Inductively Coupled Plasma Time-of-Flight Mass Spectrometry, Environ. Sci. Technol., https://doi.org/10.1021/acs.est.9b03886, 2019.

Erhardt, T., Jensen, C. M., Adolphi, F., Kjær, H. A., Dallmayr, R., Twarloh, B., Behrens, M., Hirabayashi, M., Fukuda, K., Ogata, J., Burgay, F., Scoto, F., Crotti, I., Spagnesi, A., Maffezzoli, N., Segato, D., Paleari, C., Mekhaldi, F.,

https://doi.org/10.5194/egusphere-2026-4356
Preprint. Discussion started: 18 August 2026


Muscheler, R., Darfeuil, S., and Fischer, H.: High-resolution aerosol data from the top 3.8 kyr of the East Greenland Ice coring Project (EGRIP) ice core, Earth Syst. Sci. Data, 15, 5079–5091, https://doi.org/10.5194/essd-15-5079-2023, 2023.

Evans, L. K. and Nishioka, J.: Accumulation processes of trace metals into Arctic sea ice: distribution of Fe, Mn and Cd associated with ice structure, Mar. Chem., 209, 36–47, https://doi.org/10.1016/j.marchem.2018.11.011, 2019.

Fadeev, E., Rogge, A., Ramondenc, S., Nöthig, E.-M., Wekerle, C., Bienhold, C., Salter, I., Waite, A. M., Hehemann, L., Boetius, A., and Iversen, M. H.: Sea ice presence is linked to higher carbon export and vertical microbial connectivity in the Eurasian Arctic Ocean, Commun. Biol., 4, 1255, https://doi.org/10.1038/s42003-021-02776-w, 2021.

Faïn, X., Chappellaz, J., Rhodes, R. H., Stowasser, C., Blunier, T., McConnell, J. R., Brook, E. J., Preunkert, S., Legrand, M., Debois, T., and Romanini, D.: High resolution measurements of carbon monoxide along a late Holocene Greenland ice core: evidence for in situ production, Climate of the Past, 10, 987–1000, https://doi.org/10.5194/cp-10-987-2014, 2014.

Federer, U., Kaufmann, P. R., Hutterli, M. A., Buiron, D., Blunier, T., Fischer, H., and Stocker, T. F.: A New Method for High-Resolution Methane Measurements on Polar Ice Cores Using Continuous Flow Analysis, Environ. Sci. Technol., 43, 5371–5376, https://doi.org/10.1021/es9003137, 2009.

Fountain, A. G., Campbell, J. L., Schuur, E. A. G., Stammerjohn, S. E., Williams, M. W., and Ducklow, H. W.: The Disappearing Cryosphere: Impacts and Ecosystem Responses to Rapid Cryosphere Loss, Bioscience, 62, 405–415, https://doi.org/10.1525/bio.2012.62.4.11, 2012.

Frantz, C. M., Crump, B. C., Carpenter, S., Firth, E., Orellana, M. V., Light, B., and Junge, K.: Microbial Ecology of Rotten Sea Ice: Implications for Arctic Carbon Cycling with Global Warming, Microorganisms, 14, 482, https://doi.org/10.3390/microorganisms14020482, 2026.

Fripiat, F., Sigman, D. M., Fawcett, S. E., Rafter, P. A., Weigand, M. A., and Tison, J. -L.: New insights into sea ice nitrogen biogeochemical dynamics from the nitrogen isotopes, Global Biogeochem. Cycles, 28, 115–130, https://doi.org/10.1002/2013GB004729, 2014.

Fuhrer, K., Neftel, A., Anklin, M., and Maggi, V.: Continuous measurements of hydrogen peroxide, formaldehyde, calcium and ammonium concentrations along the new grip ice core from summit, Central Greenland, Atmospheric Environment. Part A. General Topics, 27, 1873–1880, https://doi.org/10.1016/0960-1686(93)90292-7, 1993.

Geilfus, N.-X., Munson, K., Lemes, M., Wang, F., Tison, J.-L., and Rysgaard, S.: Meteoric water contribution to sea ice formation and its control of the surface water carbonate cycle on the Wandel Sea shelf, northeastern Greenland, Elementa: Science of the Anthropocene, 9, https://doi.org/10.1525/elementa.2021.00004, 2021.

https://doi.org/10.5194/egusphere-2026-4356
Preprint. Discussion started: 18 August 2026


Gkinis, V., Popp, T. J., Johnsen, S. J., and Blunier, T.: A continuous stream flash evaporator for the calibration of an IR cavity ring-down spectrometer for the isotopic analysis of water, Isotopes Environ. Health Stud., 46, 463–475, https://doi.org/10.1080/10256016.2010.538052, 2010.

Gkinis, V., Popp, T. J., Blunier, T., Bigler, M., Schüpbach, S., Kettner, E., and Johnsen, S. J.: Water isotopic ratios from a continuously melted ice core sample, Atmos. Meas. Tech., 4, 2531–2542, https://doi.org/10.5194/amt-4-2531-2011, 2011.

Golden, K. M., Ackley, S. F., and Lytle, V. I.: The Percolation Phase Transition in Sea Ice, Science (1979)., 282, 2238–2241, https://doi.org/10.1126/science.282.5397.2238, 1998.

Goto-Azuma, K., Dallmayr, R., Ogawa-Tsukagawa, Y., Moteki, N., Mori, T., Ohata, S., Kondo, Y., Koike, M., Hirabayashi, M., Ogata, J., Kitamura, K., Kawamura, K., Fujita, K., Matoba, S., Nagatsuka, N., Tsushima, A., Fukuda, K., and Aoki, T.: Technical note: High-resolution analyses of concentrations and sizes of refractory black carbon particles deposited in northwestern Greenland over the past 350 years – Part 1: Continuous flow analysis of the SIGMA-D ice core using the wide-range Single-Particle Soot Photometer and a high-efficiency nebulizer, Atmos. Chem. Phys., 24, 12985–13000, https://doi.org/10.5194/acp-24-12985-2024, 2024.

Grieman, M. M., Aydin, M., McConnell, J. R., and Saltzman, E. S.: Burning-derived vanillic acid in an Arctic ice core from Tunu, northeastern Greenland, Climate of the Past, 14, 1625–1637, https://doi.org/10.5194/cp-14-1625-2018, 2018.

Grieman, M. M., Hoffmann, H. M., Humby, J. D., Mulvaney, R., Nehrbass-Ahles, C., Rix, J., Thomas, E. R., Tuckwell, R., and Wolff, E. W.: Continuous flow analysis methods for sodium, magnesium and calcium detection in the Skytrain ice core, Journal of Glaciology, 68, 90–100, https://doi.org/10.1017/jog.2021.75, 2022.

Huber, T. M., Schwikowski, M., and Gäggeler, H. W.: Continuous melting and ion chromatographic analyses of ice cores, J. Chromatogr. A, 920, 193–200, https://doi.org/10.1016/S0021-9673(01)00613-6, 2001.

Hutchings, J. K., Heil, P., Lecomte, O., Stevens, R., Steer, A., and Lieser, J. L.: Comparing methods of measuring sea-ice density in the East Antarctic, Ann. Glaciol., 56, 77–82, https://doi.org/10.3189/2015AoG69A814, 2015.

Jones, T. R., White, J. W. C., Steig, E. J., Vaughn, B. H., Morris, V., Gkinis, V., Markle, B. R., and Schoenemann, S. W.: Improved methodologies for continuous-flow analysis of stable water isotopes in ice cores, Atmos. Meas. Tech., 10, 617–632, https://doi.org/10.5194/amt-10-617-2017, 2017.

Kaufmann, P. R., Federer, U., Hutterli, M. A., Bigler, M., Schüpbach, S., Ruth, U., Schmitt, J., and Stocker, T. F.: An Improved Continuous Flow Analysis System for High-Resolution Field Measurements on Ice Cores, Environ. Sci. Technol., 42, 8044–8050, https://doi.org/10.1021/es8007722, 2008.

Kjær, H. A., Lolk Hauge, L., Simonsen, M., Yoldi, Z., Koldtoft, I., Hörhold, M., Freitag, J., Kipfstuhl, S., Svensson, A., and Vallelonga, P.: A portable lightweight in situ analysis (LISA) box for ice and snow analysis, Cryosphere, 15, 3719–3730, https://doi.org/10.5194/tc-15-3719-2021, 2021.

https://doi.org/10.5194/egusphere-2026-4356
Preprint. Discussion started: 18 August 2026


Knüsel, S., Piguet, D. E., Schwikowski, M., and Gäggeler, H. W.: Accuracy of continuous ice-core trace-element analysis by inductively coupled plasma sector field mass spectrometry, Environ. Sci. Technol., 37, 2267–2273, https://doi.org/10.1021/es026452o, 2003.

Lange, B. A., Salganik, E., Macfarlane, A., Schneebeli, M., Høyland, K., Gardner, J., Müller, O., Divine, D. V., Kohlbach, D., Katlein, C., and Granskog, M. A.: Snowmelt contribution to Arctic first-year ice ridge mass balance and rapid consolidation during summer melt, Elem Sci Anth, 11, https://doi.org/10.1525/elementa.2022.00037, 2023.

Lannuzel, D., Bowie, A. R., van der Merwe, P. C., Townsend, A. T., and Schoemann, V.: Distribution of dissolved and particulate metals in Antarctic sea ice, Mar. Chem., 124, 134–146, https://doi.org/10.1016/j.marchem.2011.01.004, 2011.

Lannuzel, D., Vancoppenolle, M., van der Merwe, P., de Jong, J., Meiners, K. M., Grotti, M., Nishioka, J., and Schoemann, V.: Iron in sea ice: Review and new insights, Elementa: Science of the Anthropocene, 4, https://doi.org/10.12952/journal.elementa.000130, 2016.

Lenss, M., Moreau, S., Chierici, M., Claeys, P., Fransson, A., Gerland, S., Itkin, P., Osanen, J. E., Różańska-Pluta, M., Salganik, E., Wiktor, J., and Campbell, K. L.: Incorporated platelet ice layers provide refuge for sea-ice algae in the Kong Håkon VII Hav, Mar. Ecol. Prog. Ser., https://doi.org/10.3354/meps14979, 2025.

Lizotte, M. P.: The Contributions of Sea Ice Algae to Antarctic Marine Primary Production, Am. Zool., 41, 57–73, https://doi.org/10.1093/icb/41.1.57, 2001.

Martin, A. and McMinn, A.: Sea ice, extremophiles and life on extra-terrestrial ocean worlds, Int. J. Astrobiol., 17, 1–16, https://doi.org/10.1017/S1473550416000483, 2018.

Maselli, O. J., Fritzsche, D., Layman, L., McConnell, J. R., and Meyer, H.: Comparison of water isotope-ratio determinations using two cavity ring-down instruments and classical mass spectrometry in continuous ice-core analysis, Isotopes Environ. Health Stud., 49, 387–398, https://doi.org/10.1080/10256016.2013.781598, 2013.

McConnell, J. R., Lamorey, G. W., Lambert, S. W., and Taylor, K. C.: Continuous Ice-Core Chemical Analyses Using Inductively Coupled Plasma Mass Spectrometry, Environ. Sci. Technol., 36, 7–11, https://doi.org/10.1021/es011088z, 2002.

McConnell, J. R., Edwards, R., Kok, G. L., Flanner, M. G., Zender, C. S., Saltzman, E. S., Banta, J. R., Pasteris, D. R., Carter, M. M., and Kahl, J. D. W.: 20th-Century Industrial Black Carbon Emissions Altered Arctic Climate Forcing, Science (1979)., 317, 1381–1384, https://doi.org/10.1126/science.1144856, 2007.

McConnell, J. R., Burke, A., Dunbar, N. W., Köhler, P., Thomas, J. L., Arienzo, M. M., Chellman, N. J., Maselli, O. J., Sigl, M., Adkins, J. F., Baggenstos, D., Burkhart, J. F., Brook, E. J., Buizert, C., Cole-Dai, J., Fudge, T. J., Knorr, G., Graf, H.-F., Grieman, M. M., Iverson, N., McGwire, K. C., Mulvaney, R., Paris, G., Rhodes, R. H., Saltzman, E. S., Severinghaus, J. P., Steffensen, J. P., Taylor, K. C., and Winckler, G.: Synchronous volcanic eruptions and abrupt

https://doi.org/10.5194/egusphere-2026-4356
Preprint. Discussion started: 18 August 2026


climate change ~17.7 ka plausibly linked by stratospheric ozone depletion, Proceedings of the National Academy of Sciences, 114, 10035–10040, https://doi.org/10.1073/pnas.1705595114, 2017.

Meier, W. and Stroeve, J.: An Updated Assessment of the Changing Arctic Sea Ice Cover, Oceanography, https://doi.org/10.5670/oceanog.2022.114, 2022.

Miller, L. A., Fripiat, F., Else, B. G. T., Bowman, J. S., Brown, K. A., Collins, R. E., Ewert, M., Fransson, A., Gosselin, M., Lannuzel, D., Meiners, K. M., Michel, C., Nishioka, J., Nomura, D., Papadimitriou, S., Russell, L. M., Sørensen, L. L., Thomas, D. N., Tison, J.-L., van Leeuwe, M. A., Vancoppenolle, M., Wolff, E. W., and Zhou, J.: Methods for biogeochemical studies of sea ice: The state of the art, caveats, and recommendations, Elementa: Science of the Anthropocene, 3, https://doi.org/10.12952/journal.elementa.000038, 2015.

Morganti, A., Becagli, S., Castellano, E., Severi, M., Traversi, R., and Udisti, R.: An improved flow analysis–ion chromatography method for determination of cationic and anionic species at trace levels in Antarctic ice cores, Anal. Chim. Acta, 603, 190–198, https://doi.org/10.1016/j.aca.2007.09.050, 2007.

Nürnberg, D., Wollenburg, I., Dethleff, D., Eicken, H., Kassens, H., Letzig, T., Reimnitz, E., and Thiede, J.: Sediments in Arctic sea ice: Implications for entrainment, transport and release, Mar. Geol., 119, 185–214, https://doi.org/10.1016/0025-3227(94)90181-3, 1994.

Osterberg, E. C., Handley, M. J., Sneed, S. B., Mayewski, P. A., and Kreutz, K. J.: Continuous ice core melter system with discrete sampling for major ion, trace element, and stable isotope analyses, Environ. Sci. Technol., 40, 3355–3361, https://doi.org/10.1021/es052536w, 2006.

Parkinson, C. L.: A 40-y record reveals gradual Antarctic sea ice increases followed by decreases at rates far exceeding the rates seen in the Arctic, Proceedings of the National Academy of Sciences, 116, 14414–14423, https://doi.org/10.1073/pnas.1906556116, 2019.

Petrich, C. and Eicken, H.: Overview of sea ice growth and properties, in: Sea Ice, Wiley, 1–41, https://doi.org/10.1002/9781118778371.ch1, 2017.

Petteni, A., Fourré, E., Gautier, E., Spagnesi, A., Jacob, R., Akers, P. D., Zannoni, D., Gabrieli, J., Jossoud, O., Prié, F., Landais, A., Tcheng, T., Stenni, B., Savarino, J., Ginot, P., and Casado, M.: Interlaboratory comparison of continuous flow analysis (CFA) systems for high-resolution water isotope measurements in ice cores, Atmos. Meas. Tech., 18, 5435–5455, https://doi.org/10.5194/amt-18-5435-2025, 2025.

Pradel, A., Hufenus, R., Schneebeli, M., and Mitrano, D. M.: Impact of contaminant size and density on their incorporation into sea ice, Nat. Commun., 16, 4375, https://doi.org/10.1038/s41467-025-59608-2, 2025.

Reimnitz, E., McCormick, M., McDougall, K., and Brouwers, E.: Sediment Export by Ice Rafting from a Coastal Polynya, Arctic Alaska, U.S.A., Arctic and Alpine Research, 25, 83–98, https://doi.org/10.1080/00040851.1993.12002988, 1993.

https://doi.org/10.5194/egusphere-2026-4356
Preprint. Discussion started: 18 August 2026


Reimnitz, E., McCormick, M., Bischof, J., and Darby, D. A.: Comparing sea-ice sediment load with Beaufort Sea shelf deposits; is entrainment selective?, Journal of Sedimentary Research, 68, 777–787, https://doi.org/10.2110/jsr.68.777, 1998.

Rhodes, R. H., Brook, E. J., Chiang, J. C. H., Blunier, T., Maselli, O. J., McConnell, J. R., Romanini, D., and Severinghaus, J. P.: Enhanced tropical methane production in response to iceberg discharge in the North Atlantic, Science (1979)., 348, 1016–1019, https://doi.org/10.1126/science.1262005, 2015.

Röthlisberger, R., Bigler, M., Hutterli, M., Sommer, S., Stauffer, B., Junghans, H. G., and Wagenbach, D.: Technique for Continuous High-Resolution Analysis of Trace Substances in Firn and Ice Cores, Environ. Sci. Technol., 34, 338–342, https://doi.org/10.1021/es9907055, 2000.

Severi, M., Becagli, S., Traversi, R., and Udisti, R.: Recovering Paleo-Records from Antarctic Ice-Cores by Coupling a Continuous Melting Device and Fast Ion Chromatography, Anal. Chem., 87, 11441–11447, https://doi.org/10.1021/acs.analchem.5b02961, 2015.

Sigg, Andreas., Fuhrer, Katrin., Anklin, Martin., Staffelbach, Thomas., and Zurmuehle, Daniel.: A continuous analysis technique for trace species in ice cores, Environ. Sci. Technol., 28, 204–209, https://doi.org/10.1021/es00051a004, 1994.

Simonsen, M. F., Baccolo, G., Blunier, T., Borunda, A., Delmonte, B., Frei, R., Goldstein, S., Grinsted, A., Kjær, H. A., Sowers, T., Svensson, A., Vinther, B., Vladimirova, D., Winckler, G., Winstrup, M., and Vallelonga, P.: East Greenland ice core dust record reveals timing of Greenland ice sheet advance and retreat, Nat. Commun., 10, https://doi.org/10.1038/s41467-019-12546-2, 2019.

Spagnesi, A., Barbaro, E., Feltracco, M., De Blasi, F., Zannoni, D., Dreossi, G., Petteni, A., Notø, H., Lodi, R., Gabrieli, J., Holzinger, R., Gambaro, A., and Barbante, C.: An upgraded CFA – FLC – MS/MS system for the semi-continuous detection of levoglucosan in ice cores, Talanta, 265, 124799, https://doi.org/10.1016/j.talanta.2023.124799, 2023.

Steig, E. J., Jones, T. R., Schauer, A. J., Kahle, E. C., Morris, V. A., Vaughn, B. H., Davidge, L., and White, J. W. C.: Continuous-Flow Analysis of δ17O, δ18O, and δD of H2O on an Ice Core from the South Pole, Front. Earth Sci. (Lausanne)., 9, https://doi.org/10.3389/feart.2021.640292, 2021.

Stroeve, J. and Notz, D.: Changing state of Arctic sea ice across all seasons, Environmental Research Letters, 13, 103001, https://doi.org/10.1088/1748-9326/aade56, 2018.

Tedesco, L. and Vichi, M.: Sea Ice Biogeochemistry: A Guide for Modellers, PLoS One, 9, e89217, https://doi.org/10.1371/journal.pone.0089217, 2014.

Tetzner, D. R., Allen, C. S., Thomas, E. R., and Humby, J. D.: Use of excess meltwater from continuous flow analysis systems for the analysis of low concentration insoluble microparticles in ice cores, Front. Earth Sci. (Lausanne)., 13, https://doi.org/10.3389/feart.2025.1530875, 2025.

https://doi.org/10.5194/egusphere-2026-4356
Preprint. Discussion started: 18 August 2026


Thomas, E. R., Gacitúa, G., Pedro, J. B., Faith King, A. C., Markle, B., Potocki, M., and Moser, D. E.: Physical properties of shallow ice cores from Antarctic and sub-Antarctic islands, Cryosphere, 15, 1173–1186, https://doi.org/10.5194/tc-15-1173-2021, 2021.

Timco, G. W. and Frederking, R. M. W.: A review of sea ice density, Cold Reg. Sci. Technol., 24, 1–6, https://doi.org/10.1016/0165-232X(95)00007-X, 1996.

Tovar-Sánchez, A., Duarte, C. M., Alonso, J. C., Lacorte, S., Tauler, R., and Galbán-Malagón, C.: Impacts of metals and nutrients released from melting multiyear Arctic sea ice, J. Geophys. Res. Oceans, 115, https://doi.org/10.1029/2009JC005685, 2010.

Traversi, R., Becagli, S., Castellano, E., Migliori, A., Severi, M., and Udisti, R.: High-resolution fast ion chromatography (FIC) measurements of chloride, nitrate and sulphate along the EPICA Dome C ice core, Ann. Glaciol., 35, 291–298, https://doi.org/10.3189/172756402781816564, 2002.

Turner, J., Guarino, M. V., Arnatt, J., Jena, B., Marshall, G. J., Phillips, T., Bajish, C. C., Clem, K., Wang, Z., Andersson, T., Murphy, E. J., and Cavanagh, R.: Recent Decrease of Summer Sea Ice in the Weddell Sea, Antarctica, Geophys. Res. Lett., 47, https://doi.org/10.1029/2020GL087127, 2020.

Uglietti, C., Gabrielli, P., Olesik, J. W., Lutton, A., and Thompson, L. G.: Large variability of trace element mass fractions determined by ICP-SFMS in ice core samples from worldwide high altitude glaciers, Applied Geochemistry, 47, 109–121, https://doi.org/10.1016/j.apgeochem.2014.05.019, 2014.

Vallelonga, P., Maffezzoli, N., Saiz-Lopez, A., Scoto, F., Kjær, H. A., and Spolaor, A.: Sea-ice reconstructions from bromine and iodine in ice cores, Quat. Sci. Rev., 269, 107133, https://doi.org/10.1016/j.quascirev.2021.107133, 2021.

Vancoppenolle, M., Meiners, K. M., Michel, C., Bopp, L., Brabant, F., Carnat, G., Delille, B., Lannuzel, D., Madec, G., Moreau, S., Tison, J.-L., and van der Merwe, P.: Role of sea ice in global biogeochemical cycles: emerging views and challenges, Quat. Sci. Rev., 79, 207–230, https://doi.org/10.1016/j.quascirev.2013.04.011, 2013.

Wang, Q., Lu, P., Leppäranta, M., Cheng, B., Zhang, G., and Li, Z.: Physical Properties of Summer Sea Ice in the Pacific Sector of the Arctic During 2008–2018, J. Geophys. Res. Oceans, 125, https://doi.org/10.1029/2020JC016371, 2020.

Wang, S., Bailey, D., Lindsay, K., Moore, J. K., and Holland, M.: Impact of sea ice on the marine iron cycle and phytoplankton productivity, Biogeosciences, 11, 4713–4731, https://doi.org/10.5194/bg-11-4713-2014, 2014.

Wegner, C., Wittbrodt, K., Hölemann, J. A., Janout, M. A., Krumpen, T., Selyuzhenok, V., Novikhin, A., Polyakova, Ye., Krykova, I., Kassens, H., and Timokhov, L.: Sediment entrainment into sea ice and transport in the Transpolar Drift: A case study from the Laptev Sea in winter 2011/2012, Cont. Shelf Res., 141, 1–10, https://doi.org/10.1016/j.csr.2017.04.010, 2017.

https://doi.org/10.5194/egusphere-2026-4356
Preprint. Discussion started: 18 August 2026


Willis, M. D., Lannuzel, D., Else, B., Angot, H., Campbell, K., Crabeck, O., Delille, B., Hayashida, H., Lizotte, M., Loose, B., Meiners, K. M., Miller, L., Moreau, S., Nomura, D., Prytherch, J., Schmale, J., Steiner, N., Tedesco, L., and Thomas, J.: Polar oceans and sea ice in a changing climate, Elem Sci Anth, 11, https://doi.org/10.1525/elementa.2023.00056, 2023.

Winski, D. A., Osterberg, E. C., Kreutz, K. J., Ferris, D. G., Cole-Dai, J., Thundercloud, Z., Huang, J., Alexander, B., Jaeglé, L., Kennedy, J. A., Larrick, C., Kahle, E. C., Steig, E. J., and Jones, T. R.: Seasonally Resolved Holocene Sea Ice Variability Inferred From South Pole Ice Core Chemistry, Geophys. Res. Lett., 48, https://doi.org/10.1029/2020GL091602, 2021.

Winstrup, M., Vallelonga, P., Kjær, H. A., Fudge, T. J., Lee, J. E., Riis, M. H., Edwards, R., Bertler, N. A. N., Blunier, T., Brook, E. J., Buizert, C., Ciobanu, G., Conway, H., Dahl-Jensen, D., Ellis, A., Emanuelsson, B. D., Hindmarsh, R. C. A., Keller, E. D., Kurbatov, A. V., Mayewski, P. A., Neff, P. D., Pyne, R. L., Simonsen, M. F., Svensson, A., Tuohy, A., Waddington, E. D., and Wheatley, S.: A 2700-year annual timescale and accumulation history for an ice core from Roosevelt Island, West Antarctica, Climate of the Past, 15, 751–779, https://doi.org/10.5194/cp-15-751-2019, 2019.